Delft University of Technology

DIGITAL-ANALOG QUANTUM SIMULATION OF QUANTUM CHEMISTRY

Master Thesis

BY

Ignacio Fernández Graña

SUPERVISED

BY

Eliška Greplová

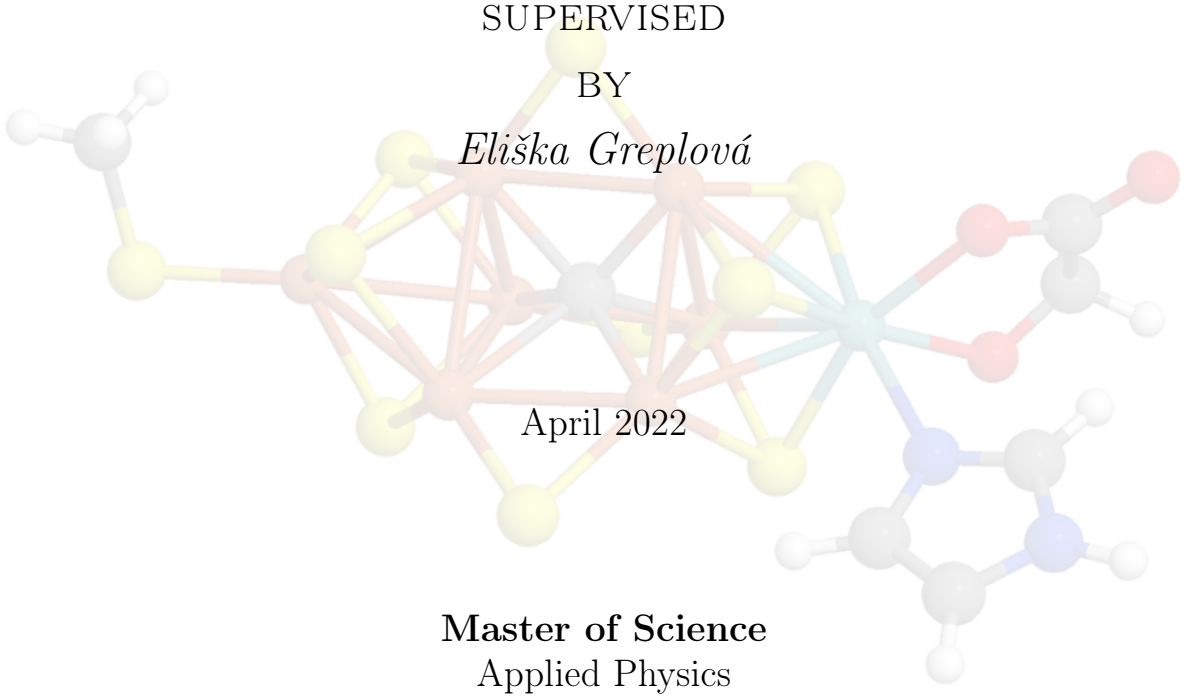

April 2022

Master of Science
Applied Physics

TU Delft Delft University of Technology

Abstract

The simulation of chemical systems and reactions is a central problem relevant to many areas of knowledge. Although a great variety of classical methods to simulate chemistry have been developed providing remarkable accuracy, some systems seem to remain intractable with classical computers. Quantum computing, on the other hand, has arised as a tool that could potentially deliver more efficient algorithms to solve relevant problems in quantum chemistry, such as the electronic structure problem. The goal of this thesis is two-fold. First, we review the three main models of quantum computation - Digital (DQC), Analog (AQC) and Adiabatic (AdQC) Quantum Computation - and their applications to quantum chemistry. Secondly, we study a recently proposed quantum computation approach which combines DQC and AQC, namely Digital-Analog Quantum Computation (DAQC). We use the DAQC model to simulate two small molecules, H_2 and HeH^+, showing that the DAQC approach outperforms the DQC for a variety of cases. We conclude by providing an overview of strategies to genelize the DAQC paradigm for larger molecules.

The code corresponding to the numerical simulations of this work
can be consulted in this repository.

Contents

A mi familia
and to those of you who made Delft worth remembering.

"I think there is a world market for maybe five computers."

Thomas Watson,
president of IBM,
1943.

1

Introduction

The simulation of quantum many-body systems is a central topic in a great variety of scientific fields. A particularly relevant quantum many-body system are molecules, which are the building blocks of most of the matter around us. Chemistry has long sought to understand how molecules, made of interacting nuclei and electrons, are formed, as well as how they interact with each others to make compounds. Understanding the properties of molecules and their reactions is a problem with applications in many fields of research, from drug discovery to materials science, medicine and energy. The birth of quantum mechanics in the early 20th century allowed for a more accurate description of molecular systems, giving rise to a new field of study known as quantum chemistry.

Soon after the birth of quantum mechanics, another technological revolution took place in the mid-20th century: the first electronic computers. Computers have had a major impact in every aspect of our society, and science, including chemistry, has greatly evolved as a consequence of the increase in our computational power. Very accurate and complex algorithms have been developed to solve quantum chemistry problems with electronic computers [1–3], providing excellent results in a great variety of cases. Nevertheless, electronic computers, which we will refer as classical computers, present some serious limitations when dealing with the simulation of quantum many-body systems [4]. One of the major challenges is that the size of the exact wavefunction of these systems grows exponentially with the number of particles, which makes it unfeasible to simulate systems of such kind for even moderate sizes.

An important class of systems where classical methods tend to fail are systems which are described by wavefunctions with a high degree of entanglement, commonly known as *strongly correlated systems*. Some relevant examples of these systems are high temperature supercon-

ductors or catalysts such as the enzyme nitrogenase, responsible for the process of nitrogen fixation. Nitrogen fixation [5] is the process of converting the non-reactive dinitrogen (N_2) in the atmosphere into more reactive compounds such as nitrates or ammonia (NH_3). Chemically speaking, this involves splitting the triple bond in N_2 to reduce it to NH_3. Nitrogen fixation is a key part of the manufacturing of fertilizer, and the main industrial method currently used for nitrogen fixation is the Haber process, developed in the early 1900s. The Haber process is very inefficient and energy-intensive, requiring very high temperatures and pressures, and it consumes around 1-2% of the world's energy supply [6]. On the other hand, there exists a type of bacteria known to be able to biologically fix the nitrogen in an very energy-efficient way, using the enzyme nitrogenase as a catalyst, at room temperature and pressure. However, the primary cofactor of the enzyme nitrogenase, FeMoco, is far beyond the simulation capabilities of our largest supercomputers, and the mechanism of nitrogen fixation at FeMoco is not yet known. However, this problem could potentially be solved by an alternative form of computation: quantum computation.

Recently, quantum computing have emerged as a novel form of computation based in the principles of quantum mechanics [7]. Quantum computers are quantum mechanical systems that can be initialized, controlled and measured to solve computational problems. The simulation of quantum many-body systems, and in particular quantum chemistry, has been identified as one of the first potential applications of quantum computers. Intuitively, it is natural to believe that using a quantum system to simulate another quantum system is more efficient than using classical computers, and quantum computers have been predicted to yield an advantage in many fields. Nevertheless, there are only a few cases where a quantum advantage has been rigorously proved, for example prime factorization using Shor's quantum algorithm, or unstructured search using Grover's quantum search algorithm. Most of the arguments towards a possible quantum advantage have been heuristic, specially in the near-term regime. This is partly due to the challenges associated with constructing and simulating quantum computers.

The majority of current computers operate under the *gate-based* quantum computation model, also refered to as Digital Quantum Computation (DQC). The basic unit of information in DQC is the qubit, a two-level controllable quantum system with states $|0\rangle$ and $|1\rangle$. A gate-based quantum computer consists of a register of n qubits, which can be acted upon with a given set of elemental quantum operations, known as quantum gates. A digital quantum algorithm is a series of quantum gates applied to the qubits, so that the system undergoes a certain evolution, which must be unitary according to the principles of quantum mechanics. We say that a quantum computer is universal if it is capable of implementing any arbitrary unitary evolution. Digital quantum computers are universal if the native gates of the device form a set of universal quantum gates.

There is currently not a preferred platform for the physical implementation of qubits, and many technologies have been proposed, including superconducting circuits [8–10], trapped ions [11], quantum dots [12], NV centers or photons [13], among others. Current digital quantum computers are still in the early experimental stages, with only tens of low-quality qubits available.

One major challenge shared by all of quantum hardware platforms is the difficulty to isolate the quantum systems making up the qubits from the environment. This leads to high rates of errors during the quantum computation, which severely limits the number of gates that can be performed in the algorithms. Quantum error correction protocols [14, 15] can protect qubits from errors, but at the expense of using a large number of qubits, which is unfeasible with the current technology. We refer to current quantum computers, with few low-quality qubits and no quantum error correction, as Noisy Intermediate Scale Quantum (NISQ) computers. Great efforts have been made in the past years in the development of digital quantum algorithms for quantum chemistry [16, 17] since the seminal work of Aspuru-Guzik *et al.* [18], both with the near-term NISQ computers and with future fault-tolerant quantum computers with access to quantum error correction. Today, there is optimism that quantum computers can solve more efficiently many problems in quantum chemistry, and the scientific community is putting great efforts towards designing new quantum algorithms with that goal.

Other paradigms of quantum computation beside the gate-based model have been developed with remarkable results. In this work we review two other quantum computational models: Analog Quantum Computation (AQC) and Adiabatic Quantum Computation (AdQC). Analog quantum computers (also called analog quantum simulators) use a controllable quantum system to simulate the physics of another less controllable quantum system [19]. An intuitive analogy is the orreries built by the ancient greeks - mechanical devices used to mimic the movement of celestial bodies [20]. The same way the orreries were designed to simulate the orbits of the planets, analog quantum simulators are engineered to simulate the physics of a specific quantum system. Quantum analog simulators typically present lower error rates and higher precision than digital quantum computers. However, unlike digital quantum computers, analog simulators are not universal in the sense that they cannot implement any unitary evolution. Analog simulators are built to study a specific system, which makes them far less flexible than digital quantum computers. Recent experiments with analog quantum simulators have demonstrated a high accuracy and low errors in the study of quantum many-body system [21, 22], gravity [23, 24] or quantum chemistry [25], among others. Most of the physics models that have been studied in analog simulators are limited to local systems with short range interactions, as it turns out to be very challenging to engineer long range interactions in most experimental platforms. However, molecules are strongly correlated systems with a long range electron-electron coulombian repulsion, and thus a full simulation of the molecular electronic structure has for long escaped analog simultations. In 2019, Argüello *et al.* [26] made the first proposal of a scalable analog quantum simulation of quantum chemistry using ultracold atoms in optical lattices. Although their proposal is still far beyond current state of the art technology, their work sets the first stone on the path towards an analog simulation of chemical systems.

The last quantum computing model we discuss is Adiabatic Quantum Computation (AdQC), introduced by Farhi *et al.* in 2000 [27]. Adiabatic quantum computers work by evolving an initial Hamiltonian, whose ground state is easy to prepare, to a more complex final Hamiltonian whose ground state encodes the solution of the computational task [28, 29]. Therefore, AdQ is

useful as long as we can encode the solution of the target problem into a Hamiltonian supported by the quantum device [30–32]. To ensure that the system ends up in the ground state of the final Hamiltonian, the evolution has to be sufficiently slow for the quantum adiabatic theorem to hold. Currently, the type of Hamiltonians supported in the quantum devices are limited to neighbours interactions. This poses a challenge for quantum chemistry applications, as the electronic Hamiltonian of molecules has long range interactions. Hamiltonian gadgets are a tool to reduce the locality of the Hamiltonian at a expense of ancilla qubits, and can be used to map the electronic Hamiltonian into a local Hamiltonian. A protocol to solve the electronic structure problem using adiabatic quantum computation and Hamiltonian gadgets was proposed in [33]. However, the number of ancilla qubits in this+ proposal scales with $N^4 \log(N)$, where N is the number of atomic orbitals required to describe the molecule, which is prohibitive for even moderate size molecules in near term devices.

Although the various models of quantum computation discussed above - DQC, AQC and AdQC - have for a long time evolved independently, recent proposals of hybrid algorithms combining different models have been done. An example of this is digitized adiabatic quantum computing, which combines the simplicity of the adiabatic algorithm with the flexibility of digital quantum computers [10, 34]. In this work, we focus on a hybrid model combining digital and analog quantum computation, which we refer to as Digital-Analog Quantum Computation (DAQC) [35–44]. The DAQC model combines the universality of DQC with the robustness of AQC against errors. It does so by substituting the two qubit gates with multi-qubit gates, which are the main source of errors in digital quantum algorithms [45, 46], with blocks of analog evolution of the interactions naturally present in the quantum hardware. In this work, we study the DAQC protocol applied to the particular case of quantum chemistry. A main challenge towards simulating quantum chemistry with the DAQC approach is the restricted locality of the natural interactions in current devices, whereas the electronic Hamiltonian presents highly non-local interactions due to the long-range electron-electron repulsion in the molecules. To circumvent this issue, a mathematical tool widely used in AdQC known as Hamiltonian gadgets [33, 47, 48] can be used. Hamiltonian gadgets work by adding auxiliary qubits to a quantum device with restricted connectivity so that the local Hamiltonian of the device simulates the non-local Hamiltonian we want to simulate.

We study the DAQC approach in small molecules that can be mapped into two-qubits, namely H_2 and HeH^+. We show these molecules can be straightforwardly mapped into a locally-connected quantum device. For these two molecules, we benchmark the DAQC, for two different tasks: finding the electronic ground state of the molecule and calculating the time dynamics of the molecule. For the ground state calculation, we use the Variational Quantum Eigensolver (VQE), a variational quantum algorithm widely used to prepare ground states of quantum many-body systems, among other tasks. On the other hand, to study the time dynamics of the molecule, we consider the time evolution of the electronic Hamiltonian using Trotter product formulas, an approximation commonly used in Hamiltonian simulation. We study these algorithms under the presence of noise, and find that the DAQC approach is more resilient to noise than the standard DQC model. However, further work is required to scale up the

simulation of quantum chemistry via the DAQC to larger molecules.

Quantum Chemistry

This chapter aims to briefly review the basics concepts of classical computational quantum chemistry. We begin, in Section 2.1, by giving an overview of the central problem in quantum chemistry, the electronic structure problem. In Section 2.2 we discuss how can the Hamiltonian of a molecule be encoded in a computer via the second quantized formalism. Last, Section 2.3 reviews the most common classical computational methods in quantum chemistry, mainly the Hartree-Fock method.

2.1 Overview

Quantum chemistry aims to understand the properties of molecules by using the formalism of quantum mechanics. The central problem in quantum chemistry is finding approximate solutions to the non-relativistic, time-independent Schrödinger equation

$$\mathcal{H}|\psi\rangle = E|\psi\rangle, \tag{2.1}$$

where $\mathcal{H}$ is the Hamiltonian of the nuclei and electrons forming the molecule. The above equation represents an eigenvalue equation, and solving it gives full information about the molecular eigenstates and eigenvalues. Besides solving this eigenvalue problem, in many settings it is also interesting to look at the non-relativistic, time-dependent Schrödinger equation

$$i\hbar\partial_t|\Psi\rangle = \mathcal{H}|\Psi\rangle \tag{2.2}$$

which dictates the time-dynamics of the molecule. It is important to note that once Eq. (2.1) is solved and the Hamiltonian is diagonalized, Eq. (2.2) becomes trivial to solve. In fact, for time-independent Hamiltonians, solving Eq. (2.2) boils down to calculating the unitary time operator $U(t) = e^{-i\hbar t\mathcal{H}}$.

An important question now arises - what does this molecular Hamiltonian $\mathcal{H}$ looks like for a general molecule? Let us consider a molecule with N_n nuclei and N_e electrons. Each nucleus $\alpha = 1, \ldots, N_n$ has a mass M_α and an atomic number Z_α, and has coordinates $\mathbf{R}_\alpha$, where we use bold letters to represent three-dimensional vectors. In an analog way, each of the N_e electrons $j = 1, \ldots, N_e$ has coordinates $\mathbf{r}_\alpha$. Then, the full molecular Hamiltonian can be written as

$$\begin{aligned}\hat{\mathcal{H}} = &-\sum_{j=1}^{N_e}\frac{1}{2}\hat{\nabla}_j^2 - \sum_{\alpha=1}^{N_n}\frac{1}{2M_\alpha}\hat{\nabla}_A^2 - \sum_{j=1}^{N_e}\sum_{\alpha=1}^{N_n}\frac{e^2}{4\pi\epsilon_0}\frac{Z_\alpha}{|\mathbf{r}_i - \mathbf{R}_\alpha|} \\ &+ \frac{1}{2}\sum_{i\neq j=1}^{N_e}\frac{e^2}{4\pi\epsilon_0}\frac{1}{|\mathbf{r}_i - \mathbf{r}_j|} + \frac{1}{2}\sum_{\alpha\neq\beta=1}^{N_e}\frac{Z_\alpha Z_\beta}{|\mathbf{R}_\alpha - \mathbf{R}_\beta|},\end{aligned} \tag{2.3}$$

where $\nabla_{j(\alpha)}$ is the Laplacian operator, involving differentiation with respect to the corresponding electronic (nuclear) coordinates, e is the electric charge of the electron and ϵ_0 is the vacuum permittivity.

A very common approximation in quantum chemistry is the so-called Born-Oppenheimer Approximation [2, 3], based on the fact that nuclei are over 1000 times heavier than electrons. Thus, nuclei can be treated as classical stationary point charges, so that the problem is expressed such that it only involves electrons moving in a stationary nuclear potential. This allows to express the wavefunctions of the nuclei and the electrons separately, greatly reducing the complexity of the problem. For the sake of clarity, from now on we work in atomic units such that the Planck constant $\hbar$, the electron mass m_e, the electron charge e and the Bohr radius a_0 are all set to 1, $\hbar = m_e = a_0 = e = 1$. In these units, the electronic Hamiltonian of a molecule under the Born-Oppenheimer approximation can then be written as

$$\mathcal{H}_e = -\sum_{j=1}^{N_e}\frac{1}{2}\hat{\nabla}_j^2 - \sum_{j=1}^{N_e}\sum_{\alpha=1}^{N_n} Z_\alpha V_c\left(\mathbf{r}_j, \mathbf{R}_\alpha\right) + \frac{1}{2}\sum_{i\neq j=1}^{N_e}\hat{V}_c\left(\mathbf{r}_i, \mathbf{r}_j\right). \tag{2.4}$$

$\hat{V}_c$ stands for a Coulomb interaction of the form $\hat{V}_c(\hat{\mathbf{r}}_1, \hat{\mathbf{r}}_2) = \frac{a}{|\hat{\mathbf{r}}_i - \hat{\mathbf{r}}_j|}$. The first term accounts for the kinetic energy of the electrons, and the second term represents the electron-nuclei attraction. The third term is the electron-electron repulsion.

Solving equations (2.1) and (2.2) for the electronic Hamiltonian $\mathcal{H}_e$ constitutes the *electronic structure problem*. Most of the work in computational quantum chemistry has focused on solving this problem. In many settings, we are only interested in solving the equations for the low lying energy eigenstates, as knowledge of the energy eigenstates allows for the prediction of reaction rates. Other typical problems in quantum chemistry involve, for example, calculating the vibrational movement of the nuclei in the molecule, among others.

2.2 Second quantization

Electrons are fermions, which means that they satisfy the Pauli exclusion principle, i.e., two identical fermions cannot occupy the same quantum state. This implies that the quantum mechanical wavefunction describing fermions must be antisymmetric with respect to exchange. The antisymmetric nature of the fermionic wavefunction can be enforced in two different ways, known as *first* and *second* quantization. The difference between the two lies in *where* this antisymmetry is enforced. First quantization imposes the antisymmetry in the *wavefunction* itself, while in second quantization it is the *operators* acting on the wavefunction which take in account the fermionic statistics of the electrons. In general, second quantization approaches are more common and have received more attention, specially within the quantum computing community, and therefore we will focus on these in this work. Nevertheless, it is worth mentioning that some important work towards first-quantized quantum algorithms has been done in the past few years [49, 50].

In order to take the electronic Hamiltonian into a second quantized formalism, we must first choose a set of N basis states, usually called *orbitals*, $\mathcal{B} = \{|\phi_p\rangle\}_{p=1}^{N}$ where to project the electronic Hamiltonian in Eq. (2.4). These basis functions approximate the electron spin-orbitals, and they define the family states $|n_1, n_2, \ldots, n_N\rangle$, where the occupation number n_p is 1 if the p-th spin-orbital is occupied and 0 if it is unoccupied. The space of all such states is known as *Fock state*. Building from this representation, one can define the creation(annihilation) fermionic operators $\hat{a}_p^\dagger(\hat{a}_p)$. These operators act on the p-th orbital as

$$\begin{aligned} \hat{a}_p|0\rangle_p &= 0, \qquad & \hat{a}_p|1\rangle_p &= |0\rangle \\ \hat{a}_p^\dagger|0\rangle_p &= |1\rangle, \qquad & \hat{a}_p^\dagger|q\rangle_p &= 0 \end{aligned} \tag{2.5}$$

Furthermore, these operators satisfy the fermionic Canonical Anticommutation Relations (CARs)

$$\{\hat{a}_p, \hat{a}_q^\dagger\} = \delta_{p,q}\hat{\mathbb{1}}, \quad \{\hat{a}_p, \hat{a}_q\} = 0 \quad \forall p, q \ , \tag{2.6}$$

If this basis $\mathcal{B}$ is complete, i.e. infinite-dimensional, then the mapping between the electronic Hamiltonian (2.4) and the second quantized picture is exact. However, for computational

purposes this basis is truncated to a finite-size, inducing a certain discretization error as a consequence of the finite-size basis. Once the set of basis functions is chosen, one can express the electronic Hamiltonian in a second quantized basis as

$$\hat{\mathcal{H}}_e = \sum_{pq} h_{pq} \hat{a}_p^\dagger \hat{a}_r + \sum_{pqrs} h_{pqrs}\ \hat{a}_p^\dagger \hat{a}_q^\dagger \hat{a}_r \hat{a}_s. \tag{2.7}$$

The first term of the above Hamiltonian captures the energy associated with the single-electron interactions, namely the electronic kinetic energy and the nuclei-electron interaction, whereas the second term encodes the electron-electron repulsion. These coefficients are calculated with the real space representation of the basis functions $\phi_p(\mathbf{r}) = \langle \mathbf{r} | \phi_p \rangle$

$$\begin{aligned} h_{pq} &= \int d\mathbf{r} \phi_p^*(\mathbf{r}) \left[-\frac{\nabla^2}{2} - \sum_\alpha Z_\alpha V_c\left(\mathbf{r}, \mathbf{R}_\alpha\right) \right] \phi_q(\mathbf{r}) \\ h_{pqrs} &= \iint d\mathbf{r} d\mathbf{r}' \phi_p^*(\mathbf{r}) \phi_q^*\left(\mathbf{r}'\right) \frac{1}{|\mathbf{r} - \mathbf{r}'|} \phi_r\left(\mathbf{r}'\right) \phi_s(\mathbf{r}) \end{aligned} \tag{2.8}$$

A typical choice for this basis functions are linear combinations of single electron spin-orbitals or *atomic orbitals*, centered around the nuclei positions. Using atomic orbitals gives a Hamiltonian with a number of terms scaling as $\mathcal{O}(N^4)$. The most common atomic orbitals is the *Slater-Type Orbitals with n Gaussians* (STO-nG basis) [2, 3], which uses n Gaussian functions to approximate the Slater determinants. Other choices of basis functions include grid basis discretization [51] or plane waves bases [52], the latter being particularly convenient for periodic systems as they enforce a periodic charge distribution. Using plane waves has the additional advantage of providing a quadratic reduction in the number of Hamiltonian terms. The choice of the orbital basis is critical for the efficiency and accuracy of the solutions. Incorporating insights from classical computational chemistry into the construction of suitable orbitals basis is key towards simulating molecules with quantum computers.

2.3 Classical algorithms

Solving the electronic structure problem is the central topic in quantum chemistry. Not only it is important by itself, but solving it is also a usual first step in algorithms developed to calculate properties of molecules and chemical reactions. The most used classical algorithm in quantum chemistry to approximate the electronic structure problem is, by far, the Hartree-Fock method [53, 54].

The Hartree-Fock (HF) method, also referred as the Self-Consistent Field (SCF) method, is a central algorithm in quantum chemistry, not only as a method itself but also as a starting point for more accurate algorithms. The HF method aims to output the best single Slater determinant

approximation to the electronic wavefunction, known as the *Hartree-Fock state*. To do so, the HF methods assumes that each electron can be described by an independent wavefunction which does not explicitly depend on the other electrons of the molecule. Each electron is described by an hydrogen-like wavefunction, and the interactions between the electrons are reduced to a mean field approximation. This is, of course, a very serious approximation, and it is the reason why HF fails to solve certain systems, particularly in strongly correlated systems where the mean-field approximation does not accurately capture the interactions.

As mentioned above, the total electronic wavefunction is described by a *Slater determinant*, which is an antisymmetrized product of atomic orbitals. Let us illustrate the concept of Slater determinant with the two-electron case. Consider a molecule with two electrons $\mathbf{x}_1$ and $\mathbf{x}_2$. The simplest ansatz one can imagine for the total electronic wavefunction $|\Psi\rangle$ is the product of the individual, separable wavefunctions of the electrons $\chi(\mathbf{x}_1)$ and $\chi(\mathbf{x}_2)$:

$$|\psi\rangle(\mathbf{x}_1, \mathbf{x}_2) = \chi_1(\mathbf{x}_1)\chi_2(\mathbf{x}_2), \tag{2.9}$$

which is known as a *Hartree product*. While this ansatz is very easy to write, it has one major shortcoming- the wavefunction is not antisymmetric! As explained in the previous section, the electronic wavefunction must be antisymmetric with respect to exchange of two electronic coordinates to satisfy the Pauli exclusion principle. The ansatz in Eq. (2.10), will in general not be antisymmetric, this is, in general $\chi_1(\mathbf{x}_1)\chi_2(\mathbf{x}_2) \neq \chi_2(\mathbf{x}_2)\chi_1(\mathbf{x}_1)$. A solution to enforce the antisymmetry in the Hartree product is known as the *Slater determinant*:

$$|\psi\rangle(\mathbf{x}_1, \mathbf{x}_2) = \frac{1}{\sqrt{2}}\left[\chi_1(\mathbf{x}_1)\chi_2(\mathbf{x}_2) - \chi_1(\mathbf{x}_2)\chi_2(\mathbf{x}_1)\right] = \frac{1}{\sqrt{2}}\begin{vmatrix}\chi_1(\mathbf{x}_1) & \chi_2(\mathbf{x}_1)\\ \chi_1(\mathbf{x}_2) & \chi_2(\mathbf{x}_2)\end{vmatrix}. \tag{2.10}$$

It is easy to see that Slater determinants are antisymmetric by construction. This concept is easily generalized to the N-electron case as

$$|\psi\rangle = \frac{1}{\sqrt{N!}}\begin{vmatrix}\chi_1(\mathbf{x}_1) & \chi_2(\mathbf{x}_1) & \cdots & \chi_N(\mathbf{x}_1)\\ \chi_1(\mathbf{x}_2) & \chi_2(\mathbf{x}_2) & \cdots & \chi_N(\mathbf{x}_2)\\ \vdots & \vdots & \ddots & \vdots\\ \chi_1(\mathbf{x}_N) & \chi_2(\mathbf{x}_N) & \cdots & \chi_N(\mathbf{x}_N)\end{vmatrix}$$

Therefore, the Hartree-Fock method outputs the best single Slater determinant approximation to the electronic wavefunction, known as the *Hartree-Fock state*. Expressing the wavefunction as this antisymmetrized product implies that the electrons interact with each other in a mean field approximation- each electron moves independently from all the others except from the average Coulomb repulsion. Electrons also feel an exchange interaction due to the symmetrization.

Although HF is able to provide a remarkably good first-approximation in many cases, it also presents severe limitations. Some relevant cases of systems where HF does not give *qualitatively* correct results is, for example, the ordering of the ionization potentials of N_2. However, the HF state is frequently used in both classical and quantum algorithms as an initial state to more refined post-HF methods. HF energy gives an upper bound to the exact energy.

The conceptually simplest classical post-HF method is the method of Configuration Interaction (CI) [2, 55, 56]. It provides an exact solution up to the inherent error due to the finite size of the orbital basis. CI uses a linear combination of all Slater determinants, optimized via a variational approach. Although it gives an exact solution, the number of required determinants grows factorially with the number of electrons and orbitals, meaning it is computationally very expensive even for moderate size systems.

The required accuracy when estimating energies to make realistic predictions is known as *chemical accuracy*, and it is normally considered to be 4kJ/mol ($1.6 \cdot 10^{-3}$ Hartree). If the energy is known to chemical accuracy, then one can predict the chemical rate of a reaction at room temperature within one order of magnitude by using Eyring equation [57]. Although classical computational chemistry can reach this accuracy in a great variety of molecular systems, there exist some relevant systems where classical computation is far from reaching this accuracy. We review in more detail how to classify the computational complexity of the electronic structure problem in Appendix (A).

3

Quantum simulation of quantum chemistry

Although many classical algorithms for quantum chemistry have been developed providing highly accurate results in many systems of interest, classical computation presents serious shortcomings when modelling some chemical systems of interest. A major challenge when simulating large molecules in classical computers is the memory required to store their wavefunction, which scales exponentially with the size. This makes unfeasible to classically simulate some relevant chemical systems and reactions, specially in the case of strongly correlated systems such as the enzyme nitrogenase responsible for nitrogen fixation, as explained in Chapter 1. Quantum computers, on the other hand, provide an exponential save in memory as they are also quantum systems with an exponentially scaling Hilbert space dimension.

In this Chapter, we review the three main models of quantum computation and their applications to quantum chemistry. We begin in Section 3.1 with the best known *gate-based* model of quantum computation, which we refer to as *Digital Quantum Computation* (DQC), and discuss digital quantum algorithms for the ground state problem (Section 3.1.2) and for time simulation (Section 3.1.3). Then, Section 3.2 discusses the concept of an analog quantum simulator and the Analog Quantum Computation (AQC) model, and reviews a recent proposal for the quantum chemistry simulation using ultracold atoms in optical lattices. Finally, ChapSectionter 3.3 describes the *Adiabatic Quantum Computation* (AdQC) model and what tools are used to map quantum many-body systems into quantum annealers with restricted connectivity.

3.1 Digital quantum computation

The first model of quantum computation we discuss is *Digital Quantum Compution* (DQC), also referred to as *gate-based* quantum computation. The basic unit of a DQC are quantum bits or *qubits*. Qubits are two-level quantum systems, normally denoted $|0\rangle$ and $|1\rangle$. Qubits can be implemented in a wide variety of physical platforms, such as for example superconducting qubits [11, 17], trapped ions [38, 58, 59], nitrogen-vacancy (NV) centers in diamonds [60], photons [61, 62] and many more. In digital quantum computing the qubits are manipulated through pre-defined quantum operations or quantum gates, which represent unitary operations acting on one or various qubits. The basic structure of a digital quantum algorithm is the following. First the qubits are initialized in an initial state that is easy to prepare, usually the state where all the qubits are in the $|0\rangle$ state. Then, a series of quantum gates are applied to the initial state, implementing a certain unitary evolution of the state of the qubits in the quantum register. Information is then retrieved from the quantum computer by measuring the state of the qubits. We say that DQC is an universal model of quantum computation as, in principle, any unitary operator can be implemented as long as the quantum computer has access to a suitable set of quantum gates. A set of quantum gates is said to be universal if any unitary operator can be decomposed in gates belonging to the set.

Current digital quantum computers still have a small number of low-quality qubits available, with low connectivity. A fundamental challenge towards realizing a large digital quantum computer is noise. Although qubits are built to be isolated from the environment, they are in practice very fragile and interact with the noisy environment. This causes qubits to decohere after short periods of time, which ultimately limits the length of the quantum algorithms that can be implemented in the quantum computer. Qubits also suffer from experimental and control errors, as their physical implementation is usually quite involved. As a way to avoid the high-rate of errors, Quantum Error Correction (QEC) methods have been proposed to encode physical qubits in more robust logical qubits by using ancillary qubits. However, the qubit requirements to have QEC in a quantum computer is still far beyond current technology. Near-term computers with no access to QEC have been coined with the term NISQ (Noisy Intermediate-Scale Quantum) computers.

Many digital quantum algorithms for quantum chemistry have been proposed in the past years [1, 63] and even implemented in real quantum hardware. In this Chapter, we distinguish two main types of digital quantum algorithms depending on whether they aim to solve the ground state problem of the molecule (i.e. solve the time-independent Schrödinger equation (2.1)) or to simulate the time-dynamics of the molecule (i.e. solve the time-dependent Schrödinger equation (2.2)). Both problems are central to quantum chemistry and a variety of algorithms have been developed to tackle them.

3.1.1 Mapping fermions into qubits

In order to encode a the second quantized electronic Hamiltonian (2.7) of a molecule in a register of qubits, we must devise a way to map fermionic operators acting on indistinguishable electrons to spin operators acting on distinguishable qubits. This mapping should, in the first place, be isospectral so that the energy spectrum of the molecule is preserved. Futhermore, it must take in account the antisymmetric nature of the electronic wavefunction: electrons in different orbitals anticommute (see CARs in 2.6), while qubits on different sites commute. Therefore, a valid fermion-to-qubit mapping should also preserve this fermionic CARs. There exist a number of methods to do this, the most of common of which we describe below.

The most basic fermion-to-qubit mapping is the Jordan-Wigner (JW) mapping. JW works by storing the occupation number of the p-th orbital in the $|0\rangle$ and $|1\rangle$ state of the p-th qubit. This means that N qubits are needed to encode N orbitals. In the JW mapping, the annihilation and creation fermionic operators are mapped into qubit operators as

$$\hat{a}_p = \left(\bigotimes_{q=0}^{p-1} Z_q\right) \sigma_p^- \qquad \text{and} \qquad \hat{a}_p^\dagger = \left(\bigotimes_{q=0}^{p-1} Z_q\right) \sigma_p^+, \tag{3.1}$$

where Z is the σ_z Pauli operator. $\sigma_p^- = |0\rangle\langle 1|_p = \frac{1}{2}(X_p + iY_p)$ and $\sigma_p^+ = |1\rangle\langle 0|_p = \frac{1}{2}(X_p - iY_p)$ are spin ladder operators satisfying $\sigma_p^-|1\rangle_p = |0\rangle_p$, $\sigma_p^+|0\rangle_p = |1\rangle_p$ and $\sigma_p^-|0\rangle_p = \sigma_p^+|1\rangle_p = 0$. The role of the string of Z operators is to preserve the fermionic anticonmmutation relations, while the ladder operators change the occupation number of the qubits. Using the JW encoding, the second quantized electronic Hamiltonian (2.7) is mapped into a k-local spin Hamiltonian

$$\mathcal{H}_e = \sum_{j=1}^{M} c_j P_j \tag{3.2}$$

where P_j are Pauli strings acting non-trivially in at most k qubits, and c_j the corresponding coefficients. The number of terms M will depend on the orbital basis set used to map the electronic Hamiltonian into the second quantized basis, and it will normally scale as $\mathcal{O}(N^4)$, being N the number of orbitals in the basis. On the other hand, the locality of the Hamiltonian k scales as $\mathcal{O}(N)$ for the JW encoding as a consequence of the Z Pauli strings in (3.3). JW therefore encodes the occupation number locally but the parity information is highly non-local. A dual mapping to JW is the parity mapping [64], which encodes the parity information locally and the occupation number non locally. The fermionic annihilation and creation operators in the parity mapping are mapped into qubit operators as

$$\hat{a}_p = Z_{p-1}\sigma_p^- \left(\bigotimes_{q=p+1}^{N} X_q\right) \qquad \text{and} \qquad \hat{a}_p^\dagger = Z_{p-1}\sigma_p^+ \left(\bigotimes_{q=p+1}^{N} X_q\right). \tag{3.3}$$

The parity mapping has the same resource requirements, using N qubits and with a locality k scaling linearly.

However, the linear scaling of the locality can be improved by using more refined fermion-to-qubit mappings. A important example is the Bravy-Kitaev (BK) mapping [65, 66], which provides qubits operators acting non-trivially on $\mathcal{O}(\log(N))$ qubits while still using N qubits to encode N orbitals. The BK mapping finds a middle ground between the JW and the parity mapping, in the sense that it encodes both the occupation number and the parity in a non-local manner. In particular, it encodes the occupation number in the even qubits, while the odd qubits store the parity of a given set of qubits. The mapping of the operators is more complex in the BK and can be found in [66].

3.1.2 Digital quantum algorithms for the ground state problem

We now discuss digital quantum algorithms to solve the electronic eigenvalue problem, this is, finding the electronic eigenstates and eigenenergies, which boils down to solving the time-independent Schrödinger equation (2.2). In many cases, we are particularly interested in finding the lowest eigenenergy, referred to as the ground state energy, and its associated eigenstate, known as the ground state. The canonical quantum algorithm to solve the eigenvalue problem is known as the Quantum Phase Estimation Algorithm (QPEA) [18, 67, 68], used to estimate the eigenvalues of an unitary operator with high probability. Unfortunately, the implementation of QPEA requires quantum circuits with depths, which is out of reach of current NISQ devices due to the short decoherence times of the qubits and the low fidelity of the gates.

Numerous alternative approaches have been developed to solve the ground state problem in NISQ devices. A particularly promising approach that has recently received a lot of attention in the literature are a set of quantum algorithms referred to as *Variational Quantum Algorithms* (VQAs). VQAs are based on a hybrid classical-quantum approach that relies on both classical and quantum computation to run the algorithms. The quantum circuit of a VQA consists of a series of *parametrized* quantum gates, whose variational parameters are optimized via a classical optimizer in order to minimize a scalar objective function. This objective function is commonly known as the *cost function* of the algorithm, and varies depending on the particular application. This way, the quantum processor is used to store the quantum wavefunction, while the classical processor is used in the optimization process.

VQAs are known to present more resilience to noise in the quantum hardware [69], which makes them an ideal candidate to achieve quantum advantage in near-term devices. Nevertheless, VQAs also presents major challenges related to trainability, as the classical optimization of the gate parameters can be a very hard problem to solve [70, 71]. One of the main difficulties of training VQAs is the emergence of regions in the training landscape where the gradient of the cost function vanishes, commonly called *barren plateaus*. In order to avoid barren plateaus it is critical to choose an ansatz adapted to the specific target problem one is trying to solve, as it

has been shown that in parametrized random circuits the probability of having barren plateaus increases exponentially with the number of qubits [72]. One of the key aspects of VQAs is that they are very versatile, and have been applied to a wide variety of problems.

An important subclass of VQAs is the *Variational Quantum Eigensolver* (VQE). Given a Hamiltonian $\mathcal{H}$ and a trial wavefunction $|\psi(\vec{\theta})\rangle$, the objective of the VQE is to provide an approximation to the ground state of the Hamiltonian, denoted by $|\psi_{gs}\rangle$, with associated ground state energy E_0. This is achieved by optimizing the parameters of the trial wavefunction, defined by the chosen parametrized quantum circuit, such that its energy $E(\vec{\theta})$ is minimized. According to the variational principle, the energy of any trial function is bounded by

$$E_0 \leq E(\vec{\theta}) = \frac{\langle\psi(\vec{\theta})|\mathcal{H}|\psi(\vec{\theta})\rangle}{\langle\psi(\vec{\theta})|\psi(\vec{\theta})\rangle}, \tag{3.4}$$

so by definition, the energy of the trial wavefunction is an upper bound of the ground state energy of $\mathcal{H}$. The associated minimization problem is defined by

$$E_{\text{VQE}} = \min_{\vec{\theta}} \langle\psi(\vec{\theta})|\mathcal{H}|\psi(\vec{\theta})\rangle. \tag{3.5}$$

Although the VQE is usually used to prepare the ground state, the algorithm can be extended to prepare excited states as well [73]. The VQE algorithm has been successfully implemented to prepare the ground state of small-size molecules in a variety of platforms [17, 58, 62]. The choice of the ansatz for the trial wavefunction, which corresponds to the parametrized quantum circuit, plays a vital role in the algorithm as it ultimately limits the expressibility of the trial wavefunction. The quality of the ansatz thus heavily conditions the accuracy of the results and the efficiency of the algorithm. If the ansatz is not general enough, it could mean that no good approximation of the ground state can be achieved by optimizing the ansatz. On the other hand, if the ansatz is not tailored to the specific problem at hand, the optimization problem associated with the VQE (Eq. 3.5) can become extremely difficult to solve, as the VQE would have to search through the whole Hilbert space of states defined by the ansatz.

There are two main approaches that can be taken to design the ansatz of a VQE. Motivated by the limited connectivity and low fidelity of the gates in NISQ devices, one can decide to use quantum circuits which take advantage of the underlying hardware where the algorithm is being run. These type of ansatze are known as *hardware efficient* (HWE) ansatze [17, 74], and most of the experimental demonstrations of the VQE so far have followed this approach, as current quantum computers are very limited in terms of quality of the qubits and gates. Given these limitations, it is convenient to use the most efficient operations available in your device for the ansatz. HWE ansatze are usually built from alternated layers of single qubit rotations and entangling blocks. However, as we mentioned previously, using random circuits not tailored to the target problem can lead to barren plateaus, which makes hardware efficient

ansatze not an escalable approach for larger circuits.

The second type of ansatz are the ones designed specifically for the target problem, usually inspired in physics-based argurments, which we refer as *physics-motivated anstaze* [75–77]. The main challenge towards practical implementations of these kind of ansatze is the deep quantum circuits they require, making their implementation unfeasible in current devices for even small molecules. Through this work, we will focus on this type of ansatz, and in particular on the Unitary Coupled-Cluster ansatz (UCC) [76–78], which is of particular importance in quantum chemistry applications. UCC is sometimes referred as the gold standard of quantum chemistry.

The UCC method is a variant of the Configurations Interaction method, where only Slater determinants with a fixed number of excitations with respect to a reference state (usually a Hartree-Fock state). The UCC ansatz is based on the Coupled Cluster operator provides the following state:

$$|\psi_{UCC}\rangle = e^{T(\vec{\theta})-T^{\dagger}(\vec{\theta})}|\phi_o\rangle, \tag{3.6}$$

with T being the anti-hermitian cluster operator:

$$T(\vec{\theta}) = \sum_k T^{(k)}(\vec{\theta}) \tag{3.7}$$

The operator $T(\vec{\theta})$ is also known as the excitation operator. The term $T^{(1)}$ generates single excitations from the reference states, $T^{(2)}$ generates double excitations, and so on. The series in Eq. (3.7) is usually truncated at second order, the *Unitary Coupled Cluster with Single and Double excitations* (UCCSD), $T(\vec{\theta}) = T^{(1)}(\vec{\theta}) + T^{(2)}(\vec{\theta})$

$$\begin{aligned} T^{(1)}(\vec{\theta}) &= \sum_{\substack{p\in \text{vir} \\ r\in \text{occ}}} \theta_p^r \hat{a}_p^{\dagger}\hat{a}_r \\ T^{(2)}(\vec{\theta}) &= \sum_{\substack{p>q\in \text{vir} \\ r>s\in \text{occ}}} \theta_{pq}^{rs}\ \hat{a}_p^{\dagger}\hat{a}_q^{\dagger}\hat{a}_r\hat{a}_s \end{aligned} \tag{3.8}$$

where *occ* and *vir* refer to occupied and virtual orbitals in the Hartree-Fock state, respectively. The UCCSD ansatz is a very common choice for the quantum circuit of the VQE algorithm, as the classical coupled cluster theory is very well studied and is among the most accurate methods for quantum chemistry simulation. Implementing the UCCSD ansatz in a quantum circuit boils down to implementing the UCC unitary operator $e^{T(\vec{\theta})-T^{\dagger}(\vec{\theta})}$ defined in Eq. (3.6). For practical applications, this unitary is normally approximated using Trotter-Suzuki formulas, which will be explained in the next section.

3.1.3 Digital quantum algorithms for time dynamics

The challenge of simulating the time evolution of the electronic Hamiltonian is of great importance in quantum chemistry. It is not only important to predict the behaviour of molecules in time, but implementing the unitary operator $U(t) = e^{i\mathcal{H}t}$ of some electronic Hamiltonian $\mathcal{H}$ is also a key subroutine of many algorithms to solve the ground state problem. This includes fault-tolerant algorithms like the Quantum Phase Estimation algorithm, but also some NISQ algorithms like the VQE algorithm with the UCC ansatz explained in the previous section.

To exactly solve the time-dependent Eq. (2.2) and implement the time-operator $U(t)$ one needs to know the full spectrum of the Hamiltonian, which becomes intractable even for small systems. Therefore, approximated methods have been developed to approximate Hamiltonian evolution. A standard approach to target this problem relies on the use of *product formulas* or *Trotterization* [9, 79–82]. Given a Hamiltonian with r terms

$$\mathcal{H} = \sum_{j=1}^{r} c_j P_j \ , \tag{3.9}$$

where P_j are Pauli strings, we want to implement an approximation of its time evolution operator $U(t) = e^{i\mathcal{H}t}$. The first order Trotter approximation of the exponential is given by

$$e^{-i\mathcal{H}t} \approx \left(\prod_{j=1}^{r} e^{-ic_j P_j t/n_T} \right)^{n_T} + \mathcal{O}\left(\sum_{j,k} [P_i, P_j] \frac{t^2}{2n_T} \right). \tag{3.10}$$

Intuitively, the above equation approximates the time operator $U(t)$ by partitioning the evolution in n_T steps, referred to as Trotter steps. In the limit where n_T is infinite, the above equation becomes exact. The error induced by the first order approximation scales with the magnitude of the commutators between all possible terms. The accuracy of the Trotterized evolution can be increased by using higher-order formulas [80, 83] and by carefully choosing the ordering strategy in which the terms $e^{-ic_j P_j t/n_T}$ are implemented [56].

3.2 Analog quantum computation

In the previous Section we have discussed the digital quantum computation paradigm, where the basic unit of information are qubits, and the algorithms are comprised of a series of quantum gates that are applied to the qubits. When it comes to the simulation of quantum mechanical systems, another quantum computation model has emerged as an important approach to study the properties and dynamics of more diverse quantum systems: *Analog Quantum Simulation* (AQS) [19, 84, 85]. The idea behind AQS is to use a controllable quantum system, the analog

simulator, to simulate another less controllable target quantum system. This is done by engineering the interactions of the target Hamiltonian in the simulator, so that the time-dynamics of the simulator corresponds with the dynamics of the simulated system. This allows to study properties of the simulated system by measuring obsevables in the simulator.

Currently available analog quantum simulators present a series of advantages with respect to their digital quantum couterparts. While digital quantum computers are still currently restricted to very small sizes up to around 100 qubits, analog simulators with up to 256 qubits have been already demonstrated [21]. Analog simulators have been used to study classically intractable spin-models [22], demonstrating quantum advantage in the analog simulation paradigm. Much like digital computers, there exists a wide variety of experimental platforms where one can implement quantum analog simulators. The most advanced architecture for analog quantum simulation is ultra-cold atoms in optical lattices [26, 86, 87], although other important possibilities include trapped ions [88], photonic simulators [13], quantum dots [12] or superconducting circuits [89], among others.

However, unlike digital quantum computers, analog simulator are specific-purpose machines which are built to solve some specific target problem. Analog quantum computers are not universal, in the sense that they cannot implement any unitary evolution of the system, and thus their application is limited to the system of study. Despite this limitation, the error rates of analog simulators are much smaller than in digital quantum computers [90], making analog simulators a strong candidate for the study of classically intractable systems [22, 91].

3.2.1 Analog simulation of quantum chemistry

Analog quantum simulators have been applied to the field of quantum chemistry, for example in the study of chemical dynamics [25], transport phenomena [92] or molecular vibrations [93]. However, a complete simulation of the electronic structure problem in an analog simulator was not proposed until very recently by Argüello *et al.* [26]. The reason behind the difficulty of building an analog simulator for quantum chemistry is the complexity of the electronic structure Hamiltonian 2.4, and in particular of the term associated with the Coulomb long-range interactions between the electrons. In a molecule, each electron interacts with every other electron according to a Coulomb potential with a $1/r$ dependency. Engineering long-range interactions in an analog simulator is a hard task, and this has been the main hurdle towards a complete simulation of the electronic structure of molecules. Indeed, most of the experimental demonstrations of analog simulations have involved local Hamiltonians, as these can be implemented in a more straightforward way.

In their seminal work [26], Arguello et al. proposed a method for engineering this long range interactions by using ulta-cold atoms in optical lattices combined with QED cavities [26]. As mentioned above, the most complex term to engineer is the electron-electron long range Coulomb repulsion, as in the optical lattice, fermionic atoms only interact locally with neighbouring

atoms. The long-range interactions between the fermionic atoms are realized by incorporating an auxiliary atomic species to the lattice, which is initialized in a Mott insulating state. This auxiliary atomic species must have three-internal long-lived states subject to different optical potentials, therefore requiring to have access to state-dependent optical potentials. Transitions between the states are mediated via a QED cavity and an external field. With these ingredients, and under a set of assumptions, it can be shown that the interaction of the fermionic atoms with the auxiliary atomic species gives rise to a $1/r$ Coulombian repulsion between the fermionic atoms mimicking the electron-electron repulsion in the molecule. Finally, the nuclear potential of the molecule is simulated via an auxiliary optical potentials, which must be shaped via 3D holographic techniques to have a Coulombian form.

Some of the above requirements for the experimental setup are out of reach with the current technology. A major challenge is that, as a consequence of using a grid discretized basis to map the electronic Hamiltonian into a second-quantized picture, a very large lattice sizes are required for the mapping to be accurate. As an example, to accurately describe the dissociation profile of the H_2 molecule, the smallest possible molecule, lattices with the order of 100x100 atoms are required [26]. Other experimental requirements that fall beyond current technology is the 3D holographic techniques needed to shape the auxiliary optical potentials simulating the nuclear potential or having access atomic state-dependent optical potential to trap the different states of the auxiliary atoms. Given the great experimental challenges building the simulator in [51], the authors proposed in an experimental pathway towards a full implementation, starting with a 2-dimensional lattice that would allow to simulate 2-dimensional molecules [51].

Besides the proposal in [26] using ultracold atoms, recently long-range electron-electron interactions were implemented in an array of gate-defined semiconductor quantum dots [94], paving the way for further quantum chemistry analog simulations in other quantum hardware platforms in the future.

3.3 Adiabatic quantum computation

The last quantum computing model we will review is *Adiabatic Quantum Computing* (AdQC) [28, 29]. AdQC is based on the fact that the solution of many computational problems can be encoded in the ground state of a quantum Hamiltonian. AdQC works by preparing the quantum device in the ground state of an initial Hamiltonian $\mathcal{H}_0$ whose ground state is easy to prepare. This initial Hamiltonian is evolved into another, more complicated Hamiltonian, $\mathcal{H}$, whose ground state encodes the solution of the computational problem. According to the quantum adiabatic theorem, if the Hamiltonian is varied sufficiently slowly, then the state of the system remains in the ground state throughout the evolution. Adiabatic quantum computation is computationally equivalent to digital quantum computation in the sense that any digital algorithm can be translated to the adiabatic model with polynomial overhead [95], and thus it is also an universal model of quantum computation . A common choice for the initial

Hamiltonian is $H_0 = -\sum_{i,j} \sigma_i^x \sigma_j^x$. This Hamiltonian is gradually reweighted according to a scheduling function $\lambda(t) \in [0, 1]$, so that $\mathcal{H}(t) = (1 - \lambda(t))\mathcal{H}_0 + \lambda(t)\mathcal{H}$ The run time of the algorithm depends on the spectral gap Δ between the ground state and the first excited state.

Quantum devices implementing the AdQC model are known as quantum annealers, and have already been used to solve various problem in optimization [30], algebra [31] and quantum simulation [32], among many others. The current state-of-the-art quantum annealing machines have around one order magnitude more qubits than state-of-the-art digital quantum computers, reaching 2000 qubits [96]. Quantum annealers have been predicted to potentially be the first quantum computing model with industrial value due to their efficiency to solve optimization problems [97], as a consequence of their current number of qubits and low levels of noise.

The first complete proposal to solve the electronic structure via AdQC was done by Babbush *et al.* [33], although other proposals to simulate quantum many-body systems in quantum annealers exist [98–102]. A major challenge when simulating quantum many-body systems in quantum annealers is the limited connectivity of the devices, which usually requires to map the target problem into an Ising model with a transverse field

$$\mathcal{H} = \sum_{i<j}^{N} g_{i,j} Z^{(i)} Z^{(j)} + \sum_i h_i X_i. \tag{3.11}$$

The electronic Hamiltonian will in general be a k-local Hamiltonian after being mapped into qubit operators (Eq. 3.2), with k scaling with the number of orbitals. The particular scaling of k will depend on the fermion-to-qubit mapping used, being $\mathcal{O}(N)$ for the Jordan-Wigner or the parity mappings, and $\log(\mathcal{O})(N)$ with the Bravyi-Kitaev mapping. Therefore, the electronic Hamiltonian cannot be mapped straightforwardly into a However, mathematical tools have been develop to map general k-local Hamiltonians into the form of Eq. (3.11). In the next Section we look at one of these mathematical tools, namely Hamiltonian gadgets.

Apart from the electronic structure problem, quantum annealers have been used to solve other problems in quantum chemistry. For instance, [103] used D-Wave quantum annealers to calculate the vibrational spectrum of two molecules, O_2 and O_3.

3.3.1 Hamiltonian gadgets

Perturbative Hamiltonian gadgets [33, 48, 104] are a mathematical technique used to embed spectra of some target non-local Hamiltonians, which in our case will be the electronic Hamiltonian 3.2, into a more restricted (normally 2-local) Hamiltonian which we refer to as *gadget* Hamiltonian $\mathcal{H}$. Hamiltonian gadgets are used simulate non-local systems, for instance quantum many-body systems, in quantum annealers with restricted (typically 2-local) interactions. Hamiltonian gadgets work by enlarging the Hilbert space of the gadget Hamiltonian, adding

a number of ancillary qubits such that the low energy spectrum of $\mathcal{H}^{gad}$ approximates the spectrum of $\mathcal{H}^{tar}$.

To introduce the idea of Hamiltonian gadget we will review here the *bit flip gadget*, introduced by Kempe *el al.* [47] in the context of proving the QMA-completeness of 2-local Hamiltonians, and later generalized in [48]. The bit flip gadget was used, with some modifications, in [33] to map the electronic Hamiltonian into a quantum annealer. It belongs to the family of *perturbative gadgets* Let us consider as the target Hamiltonian a general k-local spin Hamiltonian, which in our case will be the electronic Hamiltonian, defined as

$$\mathcal{H}^{tar} = \sum_{j=1}^{r} c_j P_j \ , \tag{3.12}$$

where P_j are Pauli strings acting non-trivially in at most k qubits,

$$P_j = \bigotimes_{j}^{k} \sigma_{s,j}, \tag{3.13}$$

with $\sigma_{s,j} = \hat{n}_{s,j} \cdot \vec{\sigma}_{s,j}$, where $\hat{n}_{s,j}$is a unit vector in $\mathbb{R}^3$ and $\vec{\sigma}_{s,j}$ is the vector of Pauli matrices acting on the j-th qubit. The goal is to simulate this Hamiltonian by using only 2-local interactions. To this end, the bit flip gadget introduces k ancilla qubits for each of the terms P_j in the Hamiltonian above, so there are rk ancilla qubits in total. Then, the gadget Hamiltonian is chosen to be

$$\mathcal{H}^{gad} = \sum_{j=1}^{r} H_s^{anc} + \lambda \sum_{j=1}^{r} V_s, \tag{3.14}$$

where the first term is the Hamiltonian of the ancilla system and the second term is a the perturbation Hamiltonian with a (small) coefficient λ, and where

$$\begin{aligned} H_s^{anc} &= \sum_{1 \le i < j \le k} \frac{1}{2} \left(I - Z_{s,i} Z_{s,j} \right) \\ V_s &= \sigma_{s,1} \otimes X_{s,1} + \sum_{j=2}^{k} c_{s,j} \sigma_{s,j} \otimes X_{s,j}. \end{aligned} \tag{3.15}$$

For each term s in the target Hamiltonian $\mathcal{H}^{tar}$ there is a corresponding register of k ancillas, and the $Z_{s,i}Z_{s,j}$ and $X_{s,j}$ terms in the equations above act on the ancilla qubits corresponding to the s term. The ancilla system has a ground state space spanned by the $|00\ldots0\rangle_{anc}$ and $|11\ldots1\rangle_{anc}$ states . On the other hand, the operator $X_s^{\otimes k} = X_{s,1} \otimes X_{s,2} \otimes \ldots \otimes X_{s,k}$ commutes

with H_{gad}, which means that $\mathcal{H}^{gad}$ can be block diagonalized into 2^r blocks correspondinng to each ancilla register ben in the +1 or -1 eigenspace of $X_s^{\otimes k}$. In [48], it was shown that the low energy eigenstates of the block corresponding to all the ancilla registers being +1, H_+^{gad}, approximate $\mathcal{H}^{tar}$. In particular, the interactions corresponding to the target Hamiltonian arise in the k-th order perturbation .

Although perturbation theory is commonly used in the creation of these gadgets, it does set high requirements in the control accuracy, as it induces a high variability in the coupling strengths, with very differences of several orders of magnitude [104, 105]. Non-pertubative gadgets which lower this control requirements have been developed for various cases [106, 107], for instance in the special case of diagonal Hamiltonians, gagdets that exactly encode the spectrum exactly have been proposed [108].

4

Digital-analog quantum simulation of quantum chemistry

In this Chapter, we review the Digital-Analog Quantum Computation (DAQC) model, which combines Analog and Digital Quantum Computation, and its applications to quantum chemistry. We begin by giving an overview of the DAQC model in Section 4.1. Section 4.2 explains what noise models we use in the simulations. Section 4.3 presents our benchmark of the DAQC approach with two-qubit molecules, H_2 and HeH^+, for the VQE algorithm and the trotterized time evolution. Finally, Section 4.4 describes strategies to scale the DAQC approach for larger molecules.

The numerical simulations for this Chapter have been done using the *Qiskit* [109], *Qutip* [110] and *PySCF* [111] packages. The full code can be consulted here.

4.1 Digital-analog quantum computation

So far in this thesis, we have discussed the three main models of quantum computation currently considered within the scientific community: digital (DQC), analog (AQC) and adiabatic (AdQC) quantum computation, each of them with their advantages and disadvantages. However, these models do not exist without overlap, and recently algorithms combining different models have been proposed. One example is digitized adiabatic quantum computing, which combines the simplicity of the adiabatic algorithm with the flexibility of digital quantum computers [10, 34]. A DAQC algorithm therefore consists of alternating layers of single-qubit gates

and two-qubit gates.

Another important example of these "hybrid"[1] algorithms belong to the so-called Digital-Analog Quantum Computation (DAQC) model [35]. The DAQ model combines the universality of DQC with the robustness of AQC against errors. A major challenge in DQC is the low fidelity of the quantum gates, which severely limits the amount of quantum gates that can be implemented in a quantum circuit. However, the fidelity of the gates is different depending on the type of gate. Although single-qubit gates (SQGs) with fidelities above 99.9% have been achieved [112], two-qubit gates (TQGs) remain the main source of errors in quantum circuits, with much lower fidelities [45]. The DAQC avoids this issue by replacing two-qubit gates by blocks of analog evolution of the underlying quantum device, which act as entangling blocks in the quantum circuits.

Previous work has succesfully showcased the DAQC methodology to implement various quantum algorithms such as the Quantum Fourier Transform [36] or the Quantum Approximate Optimization Algorithm (QAOA) [37]), as well as to simulate certain spin models [35, 38] or quantum field theories [39]. Simulation of fermionic systems such as the Hubbard model have also been proposed [40–42]. The DAQC model has also been benchmarked in IBM quantum computers using as a resource Hamiltonian the undesired cross-talk between the superconducting qubits [43].

The native Hamiltonian controlling the evolution of the analog blocks, which we refer to as the *resource* Hamiltonian, is of course dependent on the chosen quantum hardware. Most of the previous work in DAQC has considered as the resource Hamiltonian the homogeneous Ising model, as it successfully models the native Hamiltonian in various platforms. For example, the cross-resonance interaction arising in superconducting qubits can effectively be modelled by an Ising model [44]. The DAQC approach with the homogeneous Ising Hamiltonian as a resource Hamiltonian is an universal model of computation [35]. In fact, it has been proven that universal quantum computation can be achieved by using local unitaries and any two-body entangling operation [113].

In [35], a general scheme to simulate various spin models was proposed, using as a resource Hamiltonian the homogeneous Ising model

$$\mathcal{H}_r = g \sum_{j<k}^{N} Z^{(j)} Z^{(k)}. \tag{4.1}$$

Their approach used a series of alternating layer of analog evolution blocks and single qubit rotations. The central part of the procedure consists of calculating the times the analog blocks are let to evolved, which are calculated by solving a system of equations. In this work, it was

[1] In this context, "hybrid" refers to algorithms that combine different quantum computing models, not to be confused with the common use in the literature to refer to algorithms using both quantum and classical computation

shown how to simulate various spin models as the inhomogeneous Ising model, XZ model or a 4-body nearest neighbour Hamiltonian. However, the number of analog blocks needed scales exponentially with the number of terms in the Hamiltonian, meaning that for already moderate size molecules the circuit would become too deep for NISQ devices. The main challenge towards simulating quantum chemistry with the DAQC approach is the high non-locality of the electronic Hamitonian, which arises due to the long-range interactions between the electrons in a molecule, and the restricted connectivity of the natural interactions in quantum devices. This problem can be circumvent using tools to reduce the locality of the electronic Hamiltonian, as we discuss in Section 4.4.

4.2 The noise model

We now introduce the noise model we use in our simulations. Noise is one of the main challenges towards the construction of large scale quantum computers. NISQ quantum processors available today have a limited number of qubits very sensitive to various sources of errors. These qubits cannot be completely isolated, and thus they interact with the noisy environment causing errors in the computation. NISQ devices still do not have access to quantum error correction protocols, which are still on the early experimental stages [114, 115], although quantum error mitigation methods have been proposed to mitigate the noise [116]. An accurate mathematical noise model of the noise in a quantum computer is key to correctly simulate realistic quantum computations in NISQ devices.

To model noise we follow the same approach as in [117], where the DAQC model for the Quantum Fourier transform was benchmarked under the presence of noise. Following the same approach, in this work we will model noise in two different ways. Let us first start describing the control-related experimental errors, which are modelled as random phase noise in the unitary operators. The noise in single-qubit gates (SQGs), which is part of both the DQC and the DAQC models, is modelled by a random variable ξ drawn from an uniform distribution $\xi \in \mathcal{U}(1-\text{SQGN}, 1+\text{SQGN})$, where $\mathcal{U}(a,b)$ stands for an uniform distribution with boundaries (a,b). The noise in SQGs is then implemented as

$$e^{i\theta_k \sigma_j} \rightarrow e^{i\theta_k \xi \sigma_j}, \quad j = x, y, z \tag{4.2}$$

where $\sigma_j,\ j = x, y, z$ are the Pauli matrices.

In the DQC model, the entangling operation are two-qubit gates (TQGs). Following [35, 117], we model TQGs as blocks of fixed $\frac{\pi}{4}$-phase ZZ-unitaries $e^{i\frac{\pi}{4}ZZ}$ sandwiched by SQGs. For instance, a CNOT-gate with control qubit j and target qubit k is can be expressed as CNOT$= e^{i\frac{\pi}{4}Z_j} e^{-i\frac{\pi}{4}Z_j X_k} e^{i\frac{\pi}{4}X_k}$ [118]. We will use CNOTs as the TQGs in the digital circuits, but any other TQG could be decomposed into fixed-phase entangling unitaries and SQGs in

an similar way. The noise for TQGs is then modelled by a Gaussian noise in the phase of the fixed $\frac{\pi}{4}$-phase unitaries, represented by a random variable $\epsilon \in \mathcal{N}(0, \text{TQGN})$, where $\mathcal{N}(\mu, \sigma)$ stands for a Gaussian distribution with mean μ and standard deviation σ. The noise is then implemented as

$$e^{i\frac{\pi}{4}ZZ} \rightarrow e^{i\frac{\pi}{4}(1+\epsilon)ZZ} \tag{4.3}$$

Finally, in the DAQC model, noise is also introduced as a Gaussian noise in the time t are let evolved, captured by the parameter $\delta \in \mathcal{N}(0, \text{ABN})$, so that noise is implemented as

$$e^{it_\alpha \mathcal{H}_r} \rightarrow e^{i(t_\alpha+\delta)\mathcal{H}_r}. \tag{4.4}$$

Besides control related noise, we model the noise due to the interaction with the environment via the quantum channel formalism [67]. Noise processes are represented by a non-unitary channel $\mathcal{E}$ taking the density matrix of the quantum state ρ into another quantum state $\rho' = \mathcal{E}(\rho)$. This mapping must be completely-positive-trace-preserving (CPTP) in order for ρ' to be a valid quantum state. Any valid quantum channel can be written, in the operator-sum representation, as

$$\mathcal{E}(\rho) = \sum_k E_k \rho E_k^\dagger \tag{4.5}$$

where E_k are the Kraus operators defining the channel, which must satisfy $\sum_k E_k E_k^\dagger = 1$. In particular, we will use the bit-flip channel, which flips the state of a qubit from $|0\rangle$ to $|1\rangle$ with probability p_F. The Kraus operators corresponding to the bit-flip channel [67] are given by

$$E_0 = \sqrt{p_F}\mathbb{1} = \sqrt{p_F}\begin{pmatrix} 1 & 0 \\ 0 & 1 \end{pmatrix}, \qquad E_1 = \sqrt{1-p_F}X = \sqrt{1-p_F}\begin{pmatrix} 0 & 1 \\ 1 & 0 \end{pmatrix}. \tag{4.6}$$

The value of the noise parameters are taken to be SQGN=10^{-4}, TQGN=ABN=10^{-3} and $p_F = 5 \cdot 10^{-3}$.

4.3 Two-qubit molecules

We now apply the DAQC approach to the quantum chemistry case. In particular, we focus here on molecules whose electronic Hamiltonian can be mapped into 2 qubits, and thus can be expressed as

$$H_e = \sum_{\alpha,\beta=x,y,z} \nu_{1,2}^{(\alpha,\beta)} \sigma_1^{(\alpha)} \sigma_2^{(\beta)}, \tag{4.7}$$

where $\sigma_i^{(\alpha)}, \alpha = x, y, z$ represents the Pauli matrix σ^α acting on qubit i. We choose molecules of this type as the above Hamiltonian can be easily mapped into qubits that interact via an homogeneus Ising model as in Eq. (4.1). For the two-qubit case, the homogeneous Ising model reduces to

$$\mathcal{H}_{res} = \beta Z_1 Z_2, \tag{4.8}$$

which we will treat as the resource Hamiltonian. This models, for example, the kind of interaction arising in superconducting qubits [43, 44]. We study two two-qubit molecules: molecular Hydrogen (H_2) and the ion Helium Hydride (HeH^+). These molecules are among the simplest possible molecules to simulate, and have been widely studied in the context of quantum computing [59, 62–64, 119, 120], making them a suitable choice for a first benchmark of the DAQC approach for quantum chemistry.

In principle, both the H_2 and the HeH^+ molecules can be described by using 4 spin-orbitals, and therefore 4 qubits are required to map the second-quantized Hamiltonian into a qubit Hamiltonian. However, after mapping the Hamiltonian into qubit operators via the parity mapping (Section 3.1.1) one may notice that the Hamiltonian terms act trivially on two of the qubits. Therefore, the dimensionality of the problem can be reduced, converting the problem into a two-qubit Hamiltonian, as described in [64, 119]. This technique is known as *tapering* [121]. Using this reduction, the Hamiltonian for the H_2 in the STO-3G basis is given by

$$\mathcal{H}_{H_2} = \mu_0 \mathbb{1} + \mu_1 Z_1 + \mu_2 Z_2 + \mu_3 Z_1 Z_2 + \mu_4 X_1 X_2, \tag{4.9}$$

In the same STO-3G basis, the HeH^+ Hamiltonian is given by

$$\begin{aligned} \mathcal{H}_{HeH^+} =& \nu_0 \mathbb{1} + \nu_1 Z_1 + \nu_2 Z_2 + \nu_3 Z_1 Z_2 + \nu_3 Z_1 Z_2 + \nu_4 X_1 + \\ & \nu_5 X_1 Z_2 + \nu_6 X_1 Z_2 + \nu_7 X_2 + \nu_8 Z_1 X_2 + \nu_9 X_1 X_2. \end{aligned} \tag{4.10}$$

The values of the coefficients are calculated by solving the one- and two-body integrals in Eq. 2.8, which we calculated using the *Qiskit* [109] and the *PySCF* [111] packages.

4.3.1 Variational quantum eigensolver

We begin by benchmarking the DAQC approach with the Variational Quantum Eigensolver (VQE) algorithm, where we aim to find ground state energy of the H_2 and HeH^+ as accurately as possible. We choose the Unitary Coupled Cluster with Single and Double excitations (UCCSD) ansatz to design the quantum circuit. As explained in Section 3.1.2, this ansatz requires to implement the time evolution of the excitation operator $U(\vec{\theta}) = e^{T(\vec{\theta})-T^\dagger(\vec{\theta})}$. For the H_2 molecule, the UCCSSD ansatz with the parity mapping is described by

$$U(\theta)|\mathrm{HF}\rangle = e^{-i\theta X_1 Y_0}|01\rangle \tag{4.11}$$

where $|\mathrm{HF}\rangle = |01\rangle$ is the Hartree-Fock state fo H_2. This ansatz is able to exactly describe the H_2 ground state with only one variational parameter [63]. The above operator can be implemented in a digital quantum computer as shown in Figure 4.1, where we denote $e^{i\sigma_i \frac{\theta}{2}} = R_i(\theta)$, with $\sigma_i,\ i = x, y, z$ being the Pauli matrices.

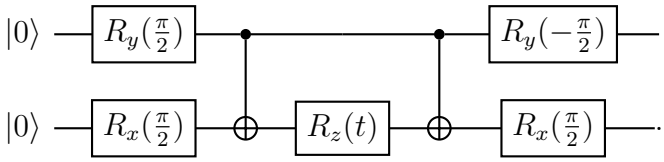

Figure 4.1: Digital circuit implementing the UCCSD-VQE ansatz for H_2 molecule.

The same circuit can, on the other hand, be simulated via the ZZ-interaction in Eq. (**??**) by realizing that the unitary $e^{itZ_1Z_2}$ can be implemented via two CNOT gates and a parametrized Z-rotation, as shown in Figure 4.2.

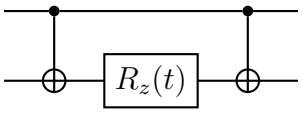

Figure 4.2: Circuit implementing $e^{itZ_1Z_2}$

The digital-analog circuit corresponding to the UCCSSD for the H_2 molecule is given in Figure 4.3, where the two-qubit gates have been substituted by an analog block.

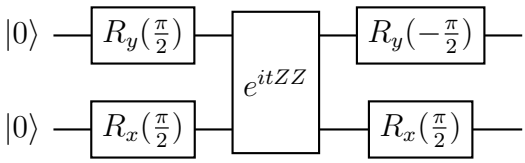

Figure 4.3: Digital-analog circuit implementing the UCCSD-VQE ansatz for the H_2 molecule.

To classically optimize the variational parameter we choose the Nelder-Mead optimizer [122, 123]. Figure (4.4) presents a comparison of the performance of the DAQC and the DQC

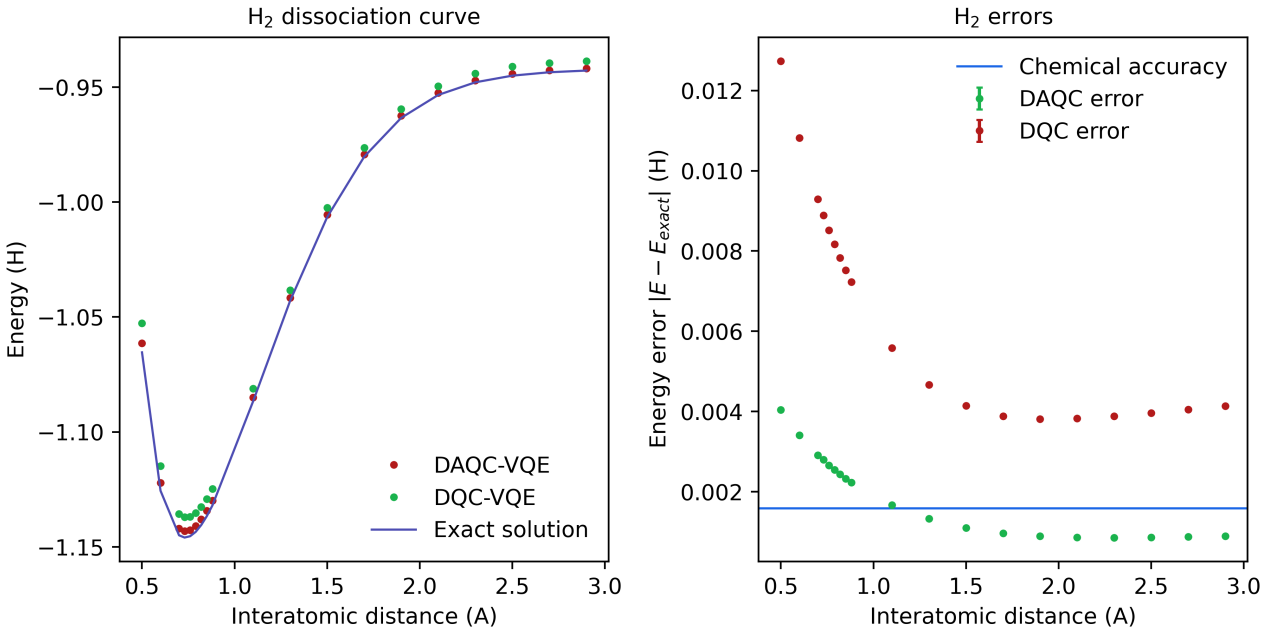

Figure 4.4: Dissociation curve of H_2 calculated through the digital (DQC) and digital-analog (DAQC) VQE for the H2 molecule with the Unitary Coupled Cluster with Single and Double excitations (UCCSD).

approaches for the UCCSD-VQE for the H_2 molecule, with the noise model described in Section 4.2 with values SQGN=10^{-4}, TQGN=ABN=10^{-3} and $p_F = 5 \cdot 10^{-3}$. As expected, the DAQC-VQE is more resilient to noise than its digital counterpart, giving energies closer to the exact solution, and even reaching chemical accuracy for interatomic distances above the equilibrium point at 0.74(A). The reason for the higher inaccuracy for distances below the equilibrium distance is probably the high inestability of the system at those distances.

The UCCSD ansatz for the HeH^+ molecule, also using the two-qubit tapering reduction, is the same as for the H_2 molecule

$$U(\theta)|\text{HF}\rangle = e^{-i\theta X_1 Y_0}|11\rangle. \tag{4.12}$$

Now the initial Hartree-Fock state corresponds to the state where both orbitals are occupied, $|\text{HF}\rangle = |11\rangle$. The results for the HeH^+ are shown in Fig. 4.5, again showing a higher resistance to noise for the DAQC approach.

4.3.2 Time dynamics

We now proceed to benchmark the DAQC and the DQC models in the context of time dynamics, solving the time-dependent Schrödinger equation (2.2). The goal is to simulate the unitary time operator $U(t) = e^{-it\mathcal{H}}$ with the electronic Hamiltonians of H_2 and HeH^+ shown in Eq. (4.9)

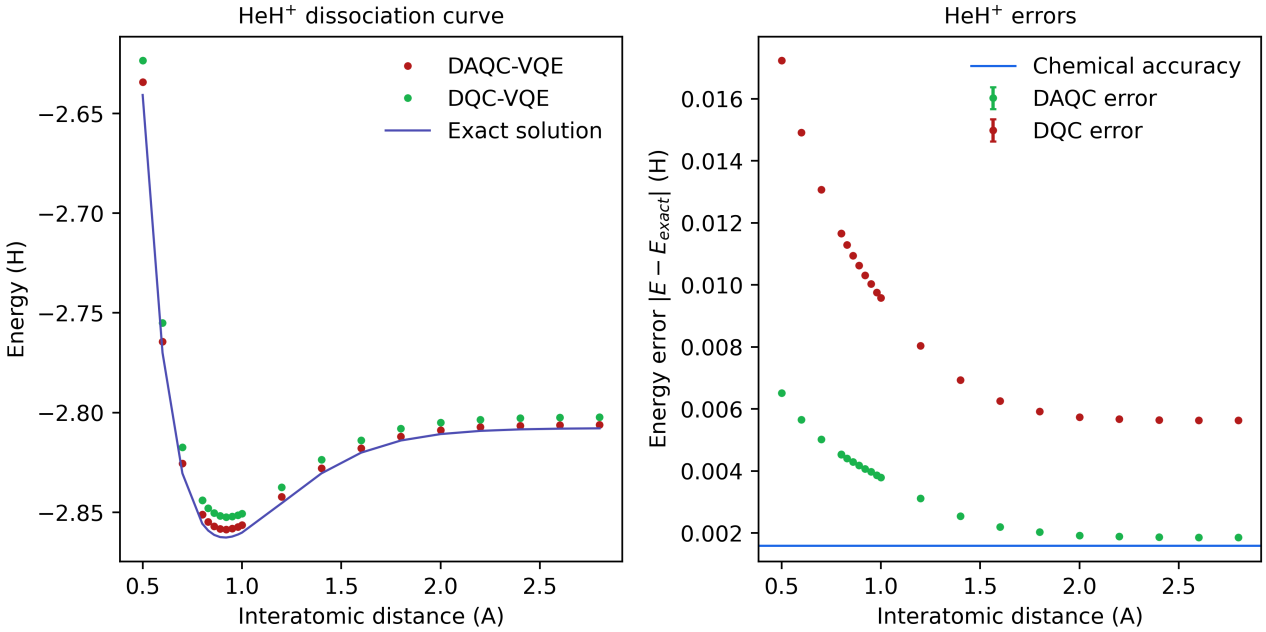

Figure 4.5: Comparison of the digital and digital-analog VQE for the HeH^+ molecule with the Unitary Coupled Cluster with Single and Double excitations (UCCSD). The energy is expressed in Hartree units and the interatomic distance between the two protons in the molecule is expressed of Amstrong ($10^{-10}m$).

and Eq. (4.10), respectively. We will implement the time operator $U(t) = e^{-it\mathcal{H}}$ via first-order trotter product formula, as explained in Section 3.1.3. This is, we will approximate the evolution of the Hamiltonians, which can expressed as $\mathcal{H} = \sum_j c_j P_j$, being P_j Pauli strings, in a series of discretized steps $e^{-i\mathcal{H}t} \approx \left(\prod_{j=1}^{r} e^{-ic_j P_j t/n_T}\right)^{n_T}$, with n_T the number of trotter steps. In the limit when $n_T \to \infty$, the previous approximation becomes exact.

For the H_2 molecule, the first-order trotterized evolution is given by

$$U(t) = e^{-i\mathcal{H}t} = \lim_{n_T \to \infty} (e^{-i\mu_1 Z_1 \frac{t}{n_T}} e^{-i\mu_2 Z_2 \frac{t}{n_T}} e^{-i\mu_3 Z_1 Z_2 \frac{t}{n_T}} e^{-i\mu_4 X_1 X_2 \frac{t}{n_T}})^{n_T}. \tag{4.13}$$

The above Hamiltonian can be simulated with access to the ZZ-interaction between the qubits in Eq. (4.8) plus single-qubit gates. The first two terms $e^{-i\mu_1 Z_1 \frac{t}{n_T}}$ and $e^{-i\mu_2 Z_2 \frac{t}{n_T}}$ are simply single qubit rotations around the Z-axis in the first and second qubits. The $e^{-i\mu_4 X_1 X_2 \frac{t}{n_T}}$ term can mapped into a e^{iZZt} analog block via single qubit rotations, by realizing that $e^{-i\frac{\pi}{4}Y} Z e^{i\frac{\pi}{4}Y} = X$. We can then write

$$e^{-i\frac{\pi}{4}Y_1} e^{-i\frac{\pi}{4}Y_2}\ e^{-iZ_1Z_2t}\ e^{i\frac{\pi}{4}Y_1} e^{i\frac{\pi}{4}Y_2} = e^{-iX_1X_2t} \tag{4.14}$$

which allows to map the trotterized evolution of the H_2 molecule into single-qubit rotations and analog blocks of ZZ-interactions. We show the corresponding circuit in Figure 4.6

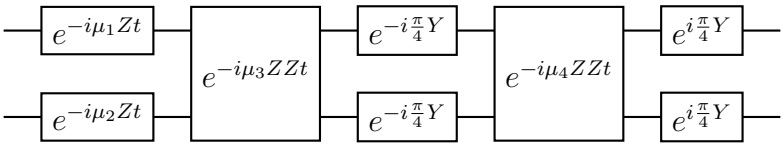

Figure 4.6: Digital-analog quantum circuit implementing a single trotter step for the H_2 molecule.

On the other hand, the trotterized evolution in Eq. (4.13) can also be implemented via DQC, with single-qubit rotations and two-qubit gates. We show an example of a digital quantum circuit implementing a single trotter step of the equation above in Figure 4.7.

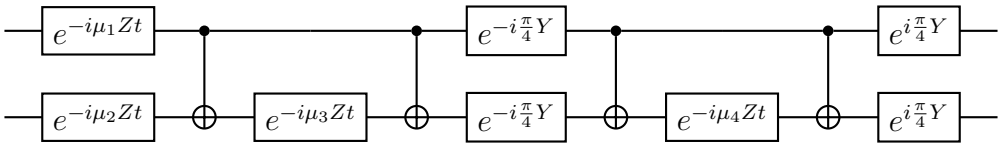

Figure 4.7: Digital quantum circuit implementing a single trotter step for the H_2 molecule.

A comparison of the performance under the presence of noise of the DAQC and the DQC approaches is shown in Fig. 4.8 for the H_2. The figure of merit we use is the fidelity with respect to the exact evolution

$$\mathcal{F}\left(\sigma_{\text{exact}}, \rho_{\text{noisy}}\right) = \left[\text{tr}\left(\sqrt{\sqrt{\sigma_{\text{exact}}}\rho_{\text{noisy}}\sqrt{\sigma_{\text{exact}}}}\right)\right]^2 \tag{4.15}$$

where σ_{exact} is the density matrix of the state after the evolution given by the exact operator $e^{-i\mathcal{H}t}$, and ρ_{noisy} the density state after the noisy DQC or DAQC circuit. We also show the fidelity of the noiseless circuit, which is the same for both DQC and DAQC, as in this case there exists an exact mapping between both. The fidelity is plotted as a function of the number of trotter steps n_T. In the noiseless case, the fidelity should increase monotonically with the number n_T. This increase is very subtle in Figure 4.8 since a single trotter step already gives a very good approximation. The reason behind this is that the H_2 Hamiltonian has only two pairs of non-commuting terms, and since the error induced by the first-order trotter evolution scales with the magnitude of the commutators between all possible terms, the accuracy of the noiseless circuit is very high already with a single trotter step. When adding noise both in the DQC and DAQC approach, the accumulation of error induce by adding more trotter steps (and thus more gates) to the circuit is greater than the improvement in the accuracy of the approximation for using more trotter steps.

An analogous procedure can be done to map the trotterized evolution of the HeH^+ Hamiltonian into a series of ZZ-analog blocks and single-qubit rotations. We plot the results for the HeH^+ in Figure 4.9, again showcasing the increased resilience to noise of the DAQC approach. In this case, the fidelity increases with the number of trotter steps for both the noiseless and the DQC circuits, as the errors induced by adding more gates is well compensated by the higher

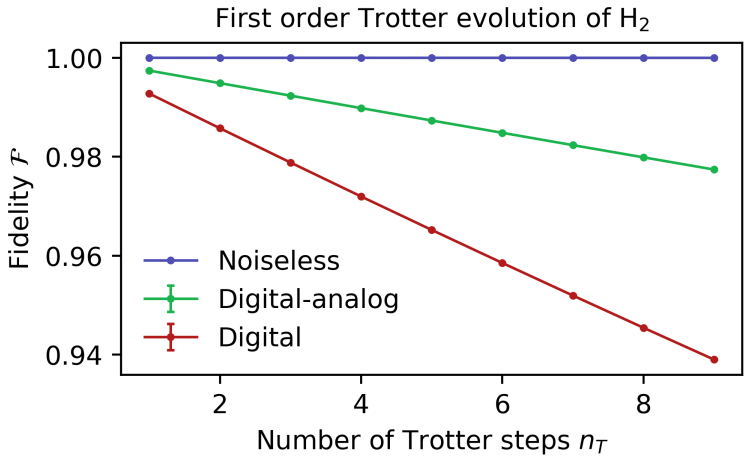

Figure 4.8: Comparison of digital and digital-analog VQE with the Unitary Coupled Cluster with Single and Double excitations (UCCSD). The Hamiltonian corresponds to the system at the equilibrium point, with an interatomic distance of 0.74 A, and it was evolved for a total time $t = 4$. The noise model $p_f = 10^{-3}$ and

accuracy of the formula for adding more trotter steps. This is not the case for the DQC circuit, so for $n_T > 3$ the fidelity starts to decrease due to the high level of noise.

One additional consideration is that turning on and off the analog interactions in the device takes in practice a finite time, which induces a certain experimental error in the circuit. As argued in previous work, an alternative approach is to not turn off the analog interactions, which has been shown to be more efficient in some cases [35, 44, 117], as the error induced by not turning off the analog interactions during the single qubit rotations was smaller than the experimental error caused by the finite time of the turning on and off the interactions.

4.4 Generalization to larger molecules

So far, we have described how to simulate two-qubit molecules in the DAQC model. However, most of the molecules of interest for quantum computation require many qubits to be modelled. Some strategies used to reduce the number of qubits is exploiting the symmetries of the molecules [124, 125] or using efficient embeddings where only the most computationally intensive tasks are done by the quantum computer [126, 127]. Howevever, these methods still require the simulation of a highly non-local electronic Hamiltonian. The main challenge towards a digital-analog simulation of larger molecules is the different locality of the native Hamiltonian in the quantum devices, which is normally limited to local interactions, and the non-local electronic Hamiltonian. One therefore needs to devise strategies to reduce the locality of the Hamiltonians, so the problem can be mapped into the restricted connectivity quantum devices available today. This problem also arises in quantum annealers, where it is commonly solved using Hamiltonian gadgets [33, 48, 105].

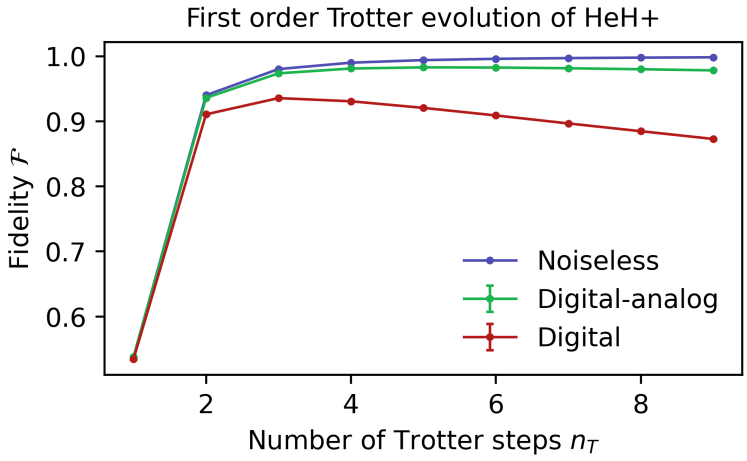

Figure 4.9: Digital vs digital-analog VQE with the Unitary Coupled Cluster with Single and Double excitations (UCCSD). The Hamiltonian corresponds to the system at equilibrium point, with an intermolecular distance $d = 0.85$, and it was evolved for a total time $t = 4$.

Hamiltonian gadgets, as described in Section 3.3.1, use auxiliary qubits to enlarge the Hilbert space of the quantum device, such that the low-energy spectrum of the effective Hamiltonian of the system simulates that of the target Hamiltonian. The main challenge towards reducing the locality with Hamiltonian gadgets is the number of ancilla qubits required to map the electronic Hamiltonian into a two-local Hamiltonian. Although the number of ancillas will depend on the particular Hamiltonian gadget, here we look at the *bit flip gadget* described in Section 3.3.1.

Let us consider that the electronic Hamiltonian is described by a k-local Hamiltonian with r terms, this is, $\mathcal{H} = \sum_{j=1}^{r} c_j P_j$, with P_j being Pauli strings acting non-trivially in at most k qubits. Then, the bit flip gadget requires rk auxiliary qubits to map the electronic Hamiltonian into a 2-local Hamiltonian. In quantum chemistry, the number of terms in the electronic Hamiltonian depends on the chosen orbital basis to map the second-quantized Hamiltonian. Usual Gaussian orbitals give Hamiltonians with $r \propto \mathcal{O}(N^4)$ terms. In addition to that, the average locality of the terms depends on the chosen fermion-to-qubit mapping. Even by using the Bravyi-Kitaev mapping, which provides a locality $k \propto \mathcal{O}(\log(N))$, the number of ancilla qubits required scales as $rk \propto N^4 \log(N)$ with the number of orbitals. This is an unfeasible requirement even for other medium size molecules. For instance, the molecule Lithium Hydride (LiH) can be mapped (by exploiting symmetries) into a four-qubit Hamiltonian with 100 terms, and thus would need the order of 400 qubits to be mapped into a local Hamiltonian. Reducing the number of terms in the Hamiltonian would greatly reduce the ancilla qubit requirements. In particular, work towards alternative choices of orbital basis other than the usual Gaussian-type orbitals has showed a quadratic reduction in the number of Hamiltonian terms by using plane-wave basis [50].

Another tool related to the idea of Hamiltonian gadget above are the so-called *local fermion-to-qubit mappings* [128–132]. Local fermion-to-qubit mappings leverage the usual fermion-to-qubit mappings, such as Jordan-Wigner or Bravyi-Kitaev, by using auxiliary qubits to reduce

the locality of the resulting spin operators to which the fermionic operators are mapped. For instance, the Cirac-Verstraete mapping [128] uses double the qubits as JW, but while JW maps local fermionic operators to spin operators acting on $\mathcal{O}(N)$ qubits, the Cirac-Verstraete is able to map local fermionic operators into local spin operators. More recent local fermion-to-qubit mappings have been proposed, optimizing both the number of qubits required per fermionic mode and the locality of the resulting spin operators [133].

5

Conclusions and future outlook

In this thesis, we have reviewed the three main models of quantum computation - digital, analog and adiabatic quantum computation - and how each of them can be applied to the specific case of quantum chemistry. We have then described the recently proposed Digital-Analog Quantum Computation model, which combines the universality of digital quantum computation with the robustness against errors of analog quantum computation. The key idea of this approach is to substitute the two-qubit gates in digital quantum circuits by blocks of analog evolution of the natural interactions present in the device. We then have applied, for the first time to our knowledge, the DAQC paradigm to the specific case of quantum chemistry by using two small molecules as a first benchmark, molecular Hydrogen H_2 and the Helium Hydride ion HeH^+.

While the molecules treated here can be straightforwardly mapped into small, locally connected quantum devices, this is not always the case, and one of the main challenges exploring DAQC approaches for larger molecules remains the high-nonlocality of the electronic Hamiltonian. We have discussed possible strategies to scale up the DAQC approach for larger molecules, and we have seen how the Hamiltonian gadget discussed in this work poses unrealistic requirements in the number of ancilla qubits needed to map the electronic Hamiltonian into a local Hamiltonian.

Further study of the strategies to reduce the locality of Hamiltonian gadgets for the specific case of DAQC is therefore needed to benchmark the true capabilities of the DAQC paradigm for quantum chemistry. Although in this work we have focused on the bit flip gadget, this gadget requires a very high number of auxiliary qubits, which indicates that more efficient methods to reduce the locality of the electronic Hamiltonian are needed. We hope this work serves as a foundation for further investigations on the digital-analog approach for quantum chemistry.

Acknowledgments

First and foremost, I would like to thank my supervisor Eliška Greplová, from whom I have learned a great deal during the eight months I have spent working on this project. Your continuous support and contagious enthusiasm for science have made this experience invaluable. I would also like to thank all the members of the QMAI group for making me feel welcomed in the group.

Completing this Masters degree would not have been possible without the company and support of my friends in Delft: Smit, Yorgos, Alberto, Matteo(s), Giulio, Pol, Erica, Eli and Gigi. These two years have been both very challenging and gratifying, and I will remember fondly my time in Delft.

Por último, quiero dar gracias a mis padres, Irene y Ángel, y a mi hermano Javi, así como al resto de mi familia, por su apoyo incondicional a lo largo de mis estudios y de mi vida.

Computational complexity theory

In this Appendix, we aim to give a brief overview of computational complexity theory and its most relevant consequences for quantum computational chemistry. Throughout this work, we have argued that many systems of interest in quantum chemistry seem to be intractable with classical computers. A natural question to ask is whether these problems are hard because their *inherent* computational difficulty or whether because we have not yet been able to find the suitable algorithms to solve them efficiently. Answering this question is crucial for the development of new efficient algorithms, as well as to know what are the inherent limits of the problems we are trying to solve. Computational complexity theory aims to shed light on these issues by classifying the problems in different *complexity classes* [134].

In general, we say a problem is efficiently solvable if for an instance of size n, there exist an algorithm that solves the problem with resources, such as time or space, scaling polynomially with n. The most basic categories of complexity classes deal with *decision problems*, this is, problems with a binary answer: "yes" or "no". If a decision problem is known to be efficiently solvable in time with a classical computer, then we say it belongs to the **P** class, which stands for *deterministic polynomial time*. The **P** class is a subclass of the more general **NP** (*non-deterministic polynomial time*) class, which contains all the problems for which, given a candidate solution, a classical computer can efficiently check if it is a solution. The question of whether a problem whose solutions can be efficiently check can also be efficiently solvable, $\mathbf{P} \stackrel{?}{=} \mathbf{NP}$, remains unanswered and constitutes one of the most important open problems in theoretical computer science. Another important class is **NP**-hard, which is defined as all the problems that are at least as hard as the hardest problems in **NP**. Problems that are both in **NP** and in **NP**-hard conform the computational class **NP**-complete. A problem being **NP**-complete is a strong evidence that there is no efficient classical algorithm to solve it.

Although the computational classes above refer to classical computation, a quantum counterpart of those also exist. The complexity class **BQP** (*bounded polynomial time*) is the quantum analog of **P**, this is, the set of problems that can be efficiently solved in quantum computer. In the same way, the analog of **NP** is the computational class **QMA** (*Quantum Merlin Arthur*), which refers to all problems such that, if given a candidate solution as a quantum state, a quantum computer can efficiently verify if it is a solution. An important note is that computational classes captures the *worst-case* hardness, and are not always representative of how difficult a problem is in practice. Many problems that are known to be **NP**-complete have very good heuristic algorithms that can approximate the solution to high accuracy efficiently. An example of this is the Hartree-Fock (HF) method, which is known to be NP-complete [135]. However, heuristic methods exist that solve the HF method in many practical cases.

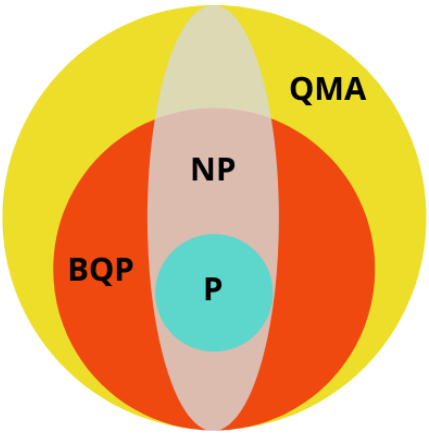

Figure A.1: Diagram summarizing the relationships between the different classical and quantum complexity classes.

Coming back to the quantum chemistry case, finding the electronic ground state of the molecular Hamiltonian (2.7) is an instance of the k-local Hamiltonian problem, which is known to be **QMA**-complete [47]. This means that in principle, it is unlikely that quantum (or classical) computers are able to exactly solve the electronic structure problem efficiently. Nevertheless, as we mentioned before, this does not mean that we cannot get a computational advantage by using quantum computers, and some heuristic methods like Variational Quantum Algorithms, explained in Chapter 3.1.2, have gained some success. A major advantage of using quantum computers is their ability to store the electronic wavefunction in the state of qubits, which in most cases is already unfeasible with classical computers. On the other hand, there are some problems in quantum chemistry that have been proved to be efficiently solved by quantum computers, this is, to **BQP** problems. Most of these are related to the simulation of the chemical time-dynamics [136, 137].

Bibliography

[1] S. McArdle, S. Endo, A. Aspuru-Guzik, S. C. Benjamin, and X. Yuan, "Quantum computational chemistry," *Reviews of Modern Physics*, vol. 92, no. 1, Mar. 2020, ISSN: 1539-0756. DOI: 10.1103/revmodphys.92.015003. [Online]. Available: http://dx.doi.org/10.1103/RevModPhys.92.015003.

[2] A. Szabo and N. S. Ostlund, *Modern Quantum Chemistry: Introduction to Advanced Electronic Structure Theory*, First. Mineola: Dover Publications, Inc., 1996.

[3] T. Helgaker, P. Jorgensen, and J. Olsen, *Molecular electronic-structure theory*. John Wiley & Sons, 2014.

[4] M. Reiher, N. Wiebe, K. M. Svore, D. Wecker, and M. Troyer, "Elucidating reaction mechanisms on quantum computers," *Proceedings of the National Academy of Sciences*, vol. 114, no. 29, pp. 7555–7560, Jul. 2017, ISSN: 1091-6490. DOI: 10.1073/pnas.1619152114. [Online]. Available: http://dx.doi.org/10.1073/pnas.1619152114.

[5] C. D. Zeinalipour-Yazdi, J. S. J. Hargreaves, and C. R. A. Catlow, "Low-t mechanisms of ammonia synthesis on co3mo3n," *The Journal of Physical Chemistry C*, vol. 122, no. 11, pp. 6078–6082, Mar. 2018, ISSN: 1932-7447. DOI: 10.1021/acs.jpcc.7b12364. [Online]. Available: https://doi.org/10.1021/acs.jpcc.7b12364.

[6] V. Smil, *Nitrogen cycle and world food production*. World Agriculture 2:9-1, 2011.

[7] R. P. Feynman, "Simulating physics with computers," *International journal of theoretical physics*, vol. 21, no. 6/7, pp. 467–488, 1982.

[8] J. Tilly *et al.*, "The variational quantum eigensolver: A review of methods and best practices," *arXiv preprint arXiv:2111.05176*, 2021.

[9] A. Smith, M. S. Kim, F. Pollmann, and J. Knolle, "Simulating quantum many-body dynamics on a current digital quantum computer," *npj Quantum Information*, vol. 5, no. 1, Nov. 2019. DOI: 10.1038/s41534-019-0217-0. [Online]. Available: https://doi.org/10.1038%2Fs41534-019-0217-0.

[10] R. Barends *et al.*, "Digitized adiabatic quantum computing with a superconducting circuit," *Nature*, vol. 534, no. 7606, pp. 222–226, Jun. 2016. DOI: 10.1038/nature17658. [Online]. Available: https://doi.org/10.1038%2Fnature17658.

[11] M.-H. Yung *et al.*, "From transistor to trapped-ion computers for quantum chemistry," *Scientific reports*, vol. 4, no. 1, pp. 1–7, 2014.

[12] X. Wang *et al.*, *Quantum simulation of an extended fermi-hubbard model using a 2d lattice of dopant-based quantum dots*, 2021. DOI: 10.48550/ARXIV.2110.08982. [Online]. Available: https://arxiv.org/abs/2110.08982.

[13] A. Aspuru-Guzik and P. Walther, "Photonic quantum simulators," *Nature Physics*, vol. 8, no. 4, pp. 285–291, Apr. 2012, ISSN: 1745-2481. DOI: 10.1038/nphys2253. [Online]. Available: https://doi.org/10.1038/nphys2253.

[14] J. Roffe, "Quantum error correction: An introductory guide," *Contemporary Physics*, vol. 60, no. 3, pp. 226–245, Jul. 2019. DOI: 10.1080/00107514.2019.1667078. [Online]. Available: https://doi.org/10.1080%2F00107514.2019.1667078.

[15] L. Egan *et al.*, *Fault-tolerant operation of a quantum error-correction code*, 2020. DOI: 10.48550/ARXIV.2009.11482. [Online]. Available: https://arxiv.org/abs/2009.11482.

[16] R. N. Tazhigulov *et al.*, *Simulating challenging correlated molecules and materials on the sycamore quantum processor*, 2022. DOI: 10.48550/ARXIV.2203.15291. [Online]. Available: https://arxiv.org/abs/2203.15291.

[17] A. Kandala *et al.*, "Hardware-efficient variational quantum eigensolver for small molecules and quantum magnets," *Nature*, vol. 549, no. 7671, pp. 242–246, Sep. 2017. DOI: 10.1038/nature23879. [Online]. Available: https://doi.org/10.1038%2Fnature23879.

[18] A. Aspuru-Guzik, A. D. Dutoi, P. J. Love, and M. Head-Gordon, "Simulated quantum computation of molecular energies," *Science*, vol. 309, no. 5741, pp. 1704–1707, Sep. 2005. DOI: 10.1126/science.1113479. [Online]. Available: https://doi.org/10.1126%2Fscience.1113479.

[19] E. Altman *et al.*, "Quantum simulators: Architectures and opportunities," *PRX Quantum*, vol. 2, p. 017003, 1 Feb. 2021. DOI: 10.1103/PRXQuantum.2.017003. [Online]. Available: https://link.aps.org/doi/10.1103/PRXQuantum.2.017003.

[20] T. Freeth, A. Jones, J. M. Steele, and Y. Bitsakis, "Calendars with olympiad display and eclipse prediction on the antikythera mechanism," *Nature*, vol. 454, no. 7204, pp. 614–617, Jul. 2008, ISSN: 1476-4687. DOI: 10.1038/nature07130. [Online]. Available: https://doi.org/10.1038/nature07130.

[21] S. Ebadi, T. T. Wang, and H. Levine, "Quantum phases of matter on a 256-atom programmable quantum simulator," *Nature*, vol. 595, no. 7866, pp. 227–232, Jul. 2021, ISSN: 1476-4687. DOI: 10.1038/s41586-021-03582-4. [Online]. Available: https://doi.org/10.1038/s41586-021-03582-4.

[22] J. Zhang *et al.*, "Observation of a many-body dynamical phase transition with a 53-qubit quantum simulator," *Nature*, vol. 551, no. 7682, pp. 601–604, Nov. 2017. DOI: 10.1038/nature24654. [Online]. Available: https://doi.org/10.1038%2Fnature24654.

[23] Z. Luo *et al.*, "Quantum simulation of the non-fermi-liquid state of sachdev-ye-kitaev model," *npj Quantum Information*, vol. 5, no. 1, p. 53, Jun. 2019, ISSN: 2056-6387. DOI: 10.1038/s41534-019-0166-7. [Online]. Available: https://doi.org/10.1038/s41534-019-0166-7.

[24] E. A. Martinez *et al.*, "Real-time dynamics of lattice gauge theories with a few-qubit quantum computer," *Nature*, vol. 534, no. 7608, pp. 516–519, Jun. 2016, ISSN: 1476-4687. DOI: 10.1038/nature18318. [Online]. Available: https://doi.org/10.1038/nature18318.

[25] R. J. MacDonell *et al.*, "Analog quantum simulation of chemical dynamics," *Chemical Science*, vol. 12, no. 28, pp. 9794–9805, 2021.

[26] J. Argüello-Luengo, A. González-Tudela, T. Shi, P. Zoller, and J. I. Cirac, "Analogue quantum chemistry simulation," *Nature*, vol. 574, no. 7777, pp. 215–218, Oct. 2019. DOI: 10.1038/s41586-019-1614-4. [Online]. Available: https://doi.org/10.1038/s41586-019-1614-4.

[27] E. Farhi, J. Goldstone, S. Gutmann, and M. Sipser, *Quantum computation by adiabatic evolution*, 2000. DOI: 10.48550/ARXIV.QUANT-PH/0001106. [Online]. Available: https://arxiv.org/abs/quant-ph/0001106.

[28] T. Albash and D. A. Lidar, "Adiabatic quantum computation," *Reviews of Modern Physics*, vol. 90, no. 1, Jan. 2018. DOI: 10.1103/revmodphys.90.015002. [Online]. Available: https://doi.org/10.1103%5C%2Frevmodphys.90.015002.

[29] N. Mohseni, P. L. McMahon, and T. Byrnes, *Ising machines as hardware solvers of combinatorial optimization problems*, 2022. DOI: 10.48550/ARXIV.2204.00276. [Online]. Available: https://arxiv.org/abs/2204.00276.

[30] I. Hen and F. M. Spedalieri, "Quantum annealing for constrained optimization," *Phys. Rev. Applied*, vol. 5, p. 034 007, 3 Mar. 2016. DOI: 10.1103/PhysRevApplied.5.034007. [Online]. Available: https://link.aps.org/doi/10.1103/PhysRevApplied.5.034007.

[31] J. C. Criado and M. Spannowsky, *Qade: Solving differential equations on quantum annealers*, 2022. DOI: 10.48550/ARXIV.2204.03657. [Online]. Available: https://arxiv.org/abs/2204.03657.

[32] A. D. King *et al.*, "Observation of topological phenomena in a programmable lattice of 1,800 qubits," *Nature*, vol. 560, no. 7719, pp. 456–460, Aug. 2018. DOI: 10.1038/s41586-018-0410-x. [Online]. Available: https://doi.org/10.1038%2Fs41586-018-0410-x.

[33] R. Babbush, P. J. Love, and A. Aspuru-Guzik, "Adiabatic quantum simulation of quantum chemistry," *Scientific reports*, vol. 4, no. 1, pp. 1–11, 2014.

[34] N. N. Hegade *et al.*, "Shortcuts to adiabaticity in digitized adiabatic quantum computing," *Physical Review Applied*, vol. 15, no. 2, Feb. 2021. DOI: 10.1103/physrevapplied.15.024038. [Online]. Available: https://doi.org/10.1103%2Fphysrevapplied.15.024038.

[35] A. Parra-Rodriguez, P. Lougovski, L. Lamata, E. Solano, and M. Sanz, "Digital-analog quantum computation," *Physical Review A*, vol. 101, no. 2, Feb. 2020, ISSN: 2469-9934. DOI: 10.1103/physreva.101.022305. [Online]. Available: http://dx.doi.org/10.1103/PhysRevA.101.022305.

[36] A. Martin, L. Lamata, E. Solano, and M. Sanz, "Digital-analog quantum algorithm for the quantum fourier transform," *Phys. Rev. Research*, vol. 2, p. 013 012, 1 Jan. 2020. DOI: 10.1103/PhysRevResearch.2.013012. [Online]. Available: https://link.aps.org/doi/10.1103/PhysRevResearch.2.013012.

[37] D. Headley, T. Müller, A. Martin, E. Solano, M. Sanz, and F. K. Wilhelm, "Approximating the quantum approximate optimisation algorithm," *arXiv preprint arXiv:2002.12215*, 2020.

[38] I. Arrazola, J. S. Pedernales, L. Lamata, and E. Solano, "Digital-analog quantum simulation of spin models in trapped ions," *Scientific Reports*, vol. 6, no. 1, p. 30 534, Jul. 2016, ISSN: 2045-2322. DOI: 10.1038/srep30534. [Online]. Available: https://doi.org/10.1038/srep30534.

[39] Z. Davoudi, N. M. Linke, and G. Pagano, "Toward simulating quantum field theories with controlled phonon-ion dynamics: A hybrid analog-digital approach," *Phys. Rev. Research*, vol. 3, p. 043 072, 4 Oct. 2021. DOI: 10.1103/PhysRevResearch.3.043072. [Online]. Available: https://link.aps.org/doi/10.1103/PhysRevResearch.3.043072.

[40] L. C. Céleri, D. Huerga, F. Albarrán-Arriagada, E. Solano, and M. Sanz, "Digital-analog quantum simulation of fermionic models," *arXiv preprint arXiv:2103.15689*, 2021.

[41] N. Guseynov and W. Pogosov, "Quantum simulation of fermionic systems using hybrid digital-analog quantum computing approach," *arXiv preprint arXiv:2112.15158*, 2021.

[42] L. Lamata, A. Parra-Rodriguez, M. Sanz, and E. Solano, "Digital-analog quantum simulations with superconducting circuits," *Advances in Physics: X*, vol. 3, no. 1, p. 1 457 981, 2018. DOI: 10.1080/23746149.2018.1457981.

[43] D. Babukhin, A. Zhukov, and W. Pogosov, "Hybrid digital-analog simulation of many-body dynamics with superconducting qubits," *Physical Review A*, vol. 101, no. 5, p. 052 337, 2020.

[44] T. Gonzalez-Raya *et al.*, "Digital-analog quantum simulations using the cross-resonance effect," *PRX Quantum*, vol. 2, p. 020 328, 2 May 2021. DOI: 10.1103/PRXQuantum.2.020328. [Online]. Available: https://link.aps.org/doi/10.1103/PRXQuantum.2.020328.

[45] C. G. Almudever *et al.*, "The engineering challenges in quantum computing," in *Design, Automation & Test in Europe Conference & Exhibition (DATE), 2017*, IEEE, 2017, pp. 836–845.

[46] M. H. Devoret, A. Wallraff, and J. M. Martinis, *Superconducting qubits: A short review*, 2004. DOI: 10.48550/ARXIV.COND-MAT/0411174. [Online]. Available: https://arxiv.org/abs/cond-mat/0411174.

[47] J. Kempe, A. Kitaev, and O. Regev, "The complexity of the local hamiltonian problem," 2004. DOI: 10.48550/ARXIV.QUANT-PH/0406180. [Online]. Available: https://arxiv.org/abs/quant-ph/0406180.

[48] S. P. Jordan and E. Farhi, "Perturbative gadgets at arbitrary orders," *Physical Review A*, vol. 77, no. 6, Jun. 2008, ISSN: 1094-1622. DOI: 10.1103/physreva.77.062329. [Online]. Available: http://dx.doi.org/10.1103/PhysRevA.77.062329.

[49] Y. Su, D. W. Berry, N. Wiebe, N. Rubin, and R. Babbush, "Fault-tolerant quantum simulations of chemistry in first quantization," *PRX Quantum*, vol. 2, no. 4, Nov. 2021. DOI: 10.1103/prxquantum.2.040332. [Online]. Available: https://doi.org/10.1103%2Fprxquantum.2.040332.

[50] R. Babbush, D. W. Berry, J. R. McClean, and H. Neven, "Quantum simulation of chemistry with sublinear scaling in basis size," *npj Quantum Information*, vol. 5, no. 1, Nov. 2019. DOI: 10.1038/s41534-019-0199-y. [Online]. Available: https://doi.org/10.1038%2Fs41534-019-0199-y.

[51] J. Argüello-Luengo, A. González-Tudela, T. Shi, P. Zoller, and J. I. Cirac, "Quantum simulation of two-dimensional quantum chemistry in optical lattices," *Phys. Rev. Research*, vol. 2, p. 042 013, 4 Oct. 2020. DOI: 10.1103/PhysRevResearch.2.042013. [Online]. Available: https://link.aps.org/doi/10.1103/PhysRevResearch.2.042013.

[52] R. Babbush, N. Wiebe, J. McClean, J. McClain, H. Neven, and G. K.-L. Chan, "Low-depth quantum simulation of materials," *Physical Review X*, vol. 8, no. 1, Mar. 2018, ISSN: 2160-3308. DOI: 10.1103/physrevx.8.011044. [Online]. Available: http://dx.doi.org/10.1103/PhysRevX.8.011044.

[53] J. C. Slater, "A simplification of the hartree-fock method," *Physical review*, vol. 81, no. 3, p. 385, 1951.

[54] D. R. Hartree and W. Hartree, "Self-consistent field, with exchange, for beryllium," *Proceedings of the Royal Society of London. Series A - Mathematical and Physical Sciences*, vol. 150, no. 869, pp. 9–33, 1935. DOI: 10.1098/rspa.1935.0085. eprint: https://royalsocietypublishing.org/doi/pdf/10.1098/rspa.1935.0085. [Online]. Available: https://royalsocietypublishing.org/doi/abs/10.1098/rspa.1935.0085.

[55] Z. Gan, D. J. Grant, R. J. Harrison, and D. A. Dixon, "The lowest energy states of the group-iiia–group-va heteronuclear diatomics: Bn, bp, aln, and alp from full configuration interaction calculations," *The Journal of chemical physics*, vol. 125, no. 12, p. 124 311, 2006.

[56] A. Tranter, P. J. Love, F. Mintert, N. Wiebe, and P. V. Coveney, "Ordering of trotterization: Impact on errors in quantum simulation of electronic structure," *Entropy*, vol. 21, no. 12, p. 1218, Dec. 2019. DOI: 10.3390/e21121218. [Online]. Available: https://doi.org/10.3390%2Fe21121218.

[57] H. Eyring, "The activated complex in chemical reactions," *The Journal of Chemical Physics*, vol. 3, no. 2, pp. 107–115, 1935. DOI: 10.1063/1.1749604. eprint: https://doi.org/10.1063/1.1749604. [Online]. Available: https://doi.org/10.1063/1.1749604.

[58] Y. Nam *et al.*, *Ground-state energy estimation of the water molecule on a trapped ion quantum computer*, 2019. DOI: 10.48550/ARXIV.1902.10171. [Online]. Available: https://arxiv.org/abs/1902.10171.

[59] C. Hempel *et al.*, "Quantum chemistry calculations on a trapped-ion quantum simulator," *Physical Review X*, vol. 8, no. 3, Jul. 2018. DOI: 10.1103/physrevx.8.031022. [Online]. Available: https://doi.org/10.1103%2Fphysrevx.8.031022.

[60] S. Pezzagna and J. Meijer, "Quantum computer based on color centers in diamond," *Applied Physics Reviews*, vol. 8, no. 1, p. 011 308, 2021.

[61] J. M. Arrazola *et al.*, "Quantum circuits with many photons on a programmable nanophotonic chip," *Nature*, vol. 591, no. 7848, pp. 54–60, Mar. 2021. DOI: 10.1038/s41586-021-03202-1. [Online]. Available: https://doi.org/10.1038%2Fs41586-021-03202-1.

[62] A. Peruzzo *et al.*, "A variational eigenvalue solver on a photonic quantum processor," *Nature Communications*, vol. 5, no. 1, Jul. 2014. DOI: 10.1038/ncomms5213. [Online]. Available: https://doi.org/10.1038%2Fncomms5213.

[63] Y. Cao, J. Romero, and J. P. Olson, "Quantum chemistry in the age of quantum computing," *Chemical Reviews*, vol. 119, no. 19, pp. 10 856–10 915, Oct. 2019, ISSN: 0009-2665. DOI: 10.1021/acs.chemrev.8b00803. [Online]. Available: https://doi.org/10.1021/acs.chemrev.8b00803.

[64] J. T. Seeley, M. J. Richard, and P. J. Love, "The bravyi-kitaev transformation for quantum computation of electronic structure," *The Journal of Chemical Physics*, vol. 137, no. 22, p. 224 109, Dec. 2012. DOI: 10.1063/1.4768229. [Online]. Available: https://doi.org/10.1063%2F1.4768229.

[65] S. B. Bravyi and A. Y. Kitaev, "Fermionic quantum computation," *Annals of Physics*, vol. 298, no. 1, pp. 210–226, May 2002. DOI: 10.1006/aphy.2002.6254. [Online]. Available: https://doi.org/10.1006%2Faphy.2002.6254.

[66] A. Tranter, P. J. Love, F. Mintert, and P. V. Coveney, "A comparison of the bravyi–kitaev and jordan–wigner transformations for the quantum simulation of quantum chemistry," *Journal of Chemical Theory and Computation*, vol. 14, no. 11, pp. 5617–5630, Sep. 2018. DOI: 10.1021/acs.jctc.8b00450. [Online]. Available: https://doi.org/10.1021%2Facs.jctc.8b00450.

[67] M. A. Nielsen and I. L. Chuang, *Quantum Computation and Quantum Information*. Cambridge University Press, 2000.

[68] A. Y. Kitaev, *Quantum measurements and the abelian stabilizer problem*, 1995. DOI: 10.48550/ARXIV.QUANT-PH/9511026. [Online]. Available: https://arxiv.org/abs/quant-ph/9511026.

[69] M. Cerezo *et al.*, "Variational quantum algorithms," *Nature Reviews Physics*, vol. 3, no. 9, pp. 625–644, Aug. 2021. DOI: 10.1038/s42254-021-00348-9. [Online]. Available: https://doi.org/10.1038%2Fs42254-021-00348-9.

[70] A. M. Childs, D. Maslov, Y. Nam, N. J. Ross, and Y. Su, "Toward the first quantum simulation with quantum speedup," *Proceedings of the National Academy of Sciences*, vol. 115, no. 38, pp. 9456–9461, Sep. 2018. DOI: 10.1073/pnas.1801723115. [Online]. Available: https://doi.org/10.1073%2Fpnas.1801723115.

[71] A. D. Corcoles *et al.*, "Challenges and opportunities of near-term quantum computing systems," *Proceedings of the IEEE*, vol. 108, no. 8, pp. 1338–1352, Aug. 2020. DOI: 10.1109/jproc.2019.2954005. [Online]. Available: https://doi.org/10.1109%2Fjproc.2019.2954005.

[72] J. R. McClean, S. Boixo, V. N. Smelyanskiy, R. Babbush, and H. Neven, "Barren plateaus in quantum neural network training landscapes," *Nature Communications*, vol. 9, no. 1, Nov. 2018. DOI: 10.1038/s41467-018-07090-4. [Online]. Available: https://doi.org/10.1038%2Fs41467-018-07090-4.

[73] J. Tilly, G. Jones, H. Chen, L. Wossnig, and E. Grant, "Computation of molecular excited states on IBM quantum computers using a discriminative variational quantum eigensolver," *Physical Review A*, vol. 102, no. 6, Dec. 2020. DOI: 10.1103/physreva.102.062425. [Online]. Available: https://doi.org/10.1103%2Fphysreva.102.062425.

[74] M. Ganzhorn *et al.*, "Gate-efficient simulation of molecular eigenstates on a quantum computer," *Phys. Rev. Applied*, vol. 11, p. 044 092, 4 Apr. 2019. DOI: 10.1103/PhysRevApplied.11.044092. [Online]. Available: https://link.aps.org/doi/10.1103/PhysRevApplied.11.044092.

[75] J. S. Kottmann and A. Aspuru-Guzik, *Optimized low-depth quantum circuits for molecular electronic structure using a separable pair approximation*, 2021. DOI: 10.48550/ARXIV.2105.03836. [Online]. Available: https://arxiv.org/abs/2105.03836.

[76] M. Kühn, S. Zanker, P. Deglmann, M. Marthaler, and H. Weiß, "Accuracy and resource estimations for quantum chemistry on a near-term quantum computer," *Journal of chemical theory and computation*, vol. 15, no. 9, pp. 4764–4780, 2019.

[77] J. Romero, R. Babbush, J. R. McClean, C. Hempel, P. Love, and A. Aspuru-Guzik, *Strategies for quantum computing molecular energies using the unitary coupled cluster ansatz*, 2017. DOI: 10.48550/ARXIV.1701.02691. [Online]. Available: https://arxiv.org/abs/1701.02691.

[78] H. R. Grimsley, D. Claudino, S. E. Economou, E. Barnes, and N. J. Mayhall, "Is the trotterized UCCSD ansatz chemically well-defined?" *Journal of Chemical Theory and Computation*, vol. 16, no. 1, pp. 1–6, Dec. 2019. DOI: 10.1021/acs.jctc.9b01083. [Online]. Available: https://doi.org/10.1021%2Facs.jctc.9b01083.

[79] P. J. Ollitrault, A. Miessen, and I. Tavernelli, "Molecular quantum dynamics: A quantum computing perspective," *Accounts of Chemical Research*, vol. 54, no. 23, pp. 4229–4238, Dec. 2021, ISSN: 0001-4842. DOI: 10.1021/acs.accounts.1c00514. [Online]. Available: https://doi.org/10.1021/acs.accounts.1c00514.

[80] L. Clinton, J. Bausch, and T. Cubitt, "Hamiltonian simulation algorithms for near-term quantum hardware," *Nature Communications*, vol. 12, no. 1, Aug. 2021. DOI: 10.1038/s41467-021-25196-0. [Online]. Available: https://doi.org/10.1038%2Fs41467-021-25196-0.

[81] S. Lloyd, "Universal quantum simulators," *Science*, vol. 273, no. 5278, pp. 1073–1078, 1996. DOI: 10.1126/science.273.5278.1073. eprint: https://www.science.org/doi/pdf/10.1126/science.273.5278.1073. [Online]. Available: https://www.science.org/doi/abs/10.1126/science.273.5278.1073.

[82] A. M. Childs, Y. Su, M. C. Tran, N. Wiebe, and S. Zhu, "Theory of trotter error with commutator scaling," *Phys. Rev. X*, vol. 11, p. 011 020, 1 Feb. 2021. DOI: 10.1103/PhysRevX.11.011020. [Online]. Available: https://link.aps.org/doi/10.1103/PhysRevX.11.011020.

[83] M. Motta *et al.*, *Low rank representations for quantum simulation of electronic structure*, 2018. DOI: 10.48550/ARXIV.1808.02625. [Online]. Available: https://arxiv.org/abs/1808.02625.

[84] I. M. Georgescu, S. Ashhab, and F. Nori, "Quantum simulation," *Rev. Mod. Phys.*, vol. 86, pp. 153–185, 1 Mar. 2014. DOI: 10.1103/RevModPhys.86.153. [Online]. Available: https://link.aps.org/doi/10.1103/RevModPhys.86.153.

[85] T. H. Johnson, S. R. Clark, and D. Jaksch, "What is a quantum simulator?" *EPJ Quantum Technology*, vol. 1, no. 1, pp. 1–12, 2014.

[86] D. Jaksch and P. Zoller, "The cold atom hubbard toolbox," *Annals of physics*, vol. 315, no. 1, pp. 52–79, 2005.

[87] F. Schäfer, T. Fukuhara, S. Sugawa, Y. Takasu, and Y. Takahashi, "Tools for quantum simulation with ultracold atoms in optical lattices," *Nature Reviews Physics*, vol. 2, no. 8, pp. 411–425, Jul. 2020. DOI: 10.1038/s42254-020-0195-3. [Online]. Available: https://doi.org/10.1038%2Fs42254-020-0195-3.

[88] J. W. Britton *et al.*, "Engineered two-dimensional ising interactions in a trapped-ion quantum simulator with hundreds of spins," *Nature*, vol. 484, no. 7395, pp. 489–492, Apr. 2012. DOI: 10.1038/nature10981. [Online]. Available: https://doi.org/10.1038%2Fnature10981.

[89] Y. Yanay, J. Braumüller, T. P. Orlando, S. Gustavsson, C. Tahan, and W. D. Oliver, "Mediated interactions beyond the nearest neighbor in an array of superconducting qubits," *Physical Review Applied*, vol. 17, no. 3, Mar. 2022. DOI: 10.1103/physrevapplied.17.034060. [Online]. Available: https://doi.org/10.1103%2Fphysrevapplied.17.034060.

[90] P. M. Poggi, N. K. Lysne, K. W. Kuper, I. H. Deutsch, and P. S. Jessen, "Quantifying the sensitivity to errors in analog quantum simulation," *PRX Quantum*, vol. 1, p. 020 308, 2 Nov. 2020. DOI: 10.1103/PRXQuantum.1.020308. [Online]. Available: https://link.aps.org/doi/10.1103/PRXQuantum.1.020308.

[91] J. Eisert, M. Friesdorf, and C. Gogolin, "Quantum many-body systems out of equilibrium," *Nature Physics*, vol. 11, no. 2, pp. 124–130, Feb. 2015, ISSN: 1745-2481. DOI: 10.1038/nphys3215. [Online]. Available: http://dx.doi.org/10.1038/nphys3215.

[92] L. Garcıa-Álvarez, U. Las Heras, A. Mezzacapo, M. Sanz, E. Solano, and L. Lamata, "Quantum chemistry and charge transport in biomolecules with superconducting circuits," *Scientific reports*, vol. 6, no. 1, pp. 1–9, 2016.

[93] R. Gobato and A. Heidari, "Calculations using quantum chemistry for inorganic molecule simulation beli2sesi," *American Journal of Quantum Chemistry and Molecular Spectroscopy*, vol. 2, no. 3, pp. 37–46, 2017.

[94] J. Knörzer *et al.*, *Long-range electron-electron interactions in quantum dot systems and applications in quantum chemistry*, 2022. DOI: 10.48550/ARXIV.2202.06756. [Online]. Available: https://arxiv.org/abs/2202.06756.

[95] D. Aharonov, W. van Dam, J. Kempe, Z. Landau, S. Lloyd, and O. Regev, "Adiabatic quantum computation is equivalent to standard quantum computation," 2004. DOI: 10.48550/ARXIV.QUANT-PH/0405098. [Online]. Available: https://arxiv.org/abs/quant-ph/0405098.

[96] A. D. King *et al.*, *Coherent quantum annealing in a programmable 2000-qubit ising chain*, 2022. DOI: 10.48550/ARXIV.2202.05847. [Online]. Available: https://arxiv.org/abs/2202.05847.

[97] A. Perdomo-Ortiz *et al.*, "Readiness of quantum optimization machines for industrial applications," *Physical Review Applied*, vol. 12, no. 1, Jul. 2019. DOI: 10.1103/physrevapplied.12.014004. [Online]. Available: https://doi.org/10.1103%2Fphysrevapplied.12.014004.

[98] M. Streif, F. Neukart, and M. Leib, *Solving quantum chemistry problems with a d-wave quantum annealer*, 2018. DOI: 10.48550/ARXIV.1811.05256. [Online]. Available: https://arxiv.org/abs/1811.05256.

[99] R. Xia, T. Bian, and S. Kais, *Electronic structure calculations and the ising hamiltonian*, 2017. DOI: 10.48550/ARXIV.1706.00271. [Online]. Available: https://arxiv.org/abs/1706.00271.

[100] A. Perdomo, C. Truncik, I. Tubert-Brohman, G. Rose, and A. Aspuru-Guzik, "Construction of model hamiltonians for adiabatic quantum computation and its application to finding low-energy conformations of lattice protein models," *Physical Review A*, vol. 78, no. 1, p. 012 320, 2008.

[101] M. Leib, P. Zoller, and W. Lechner, *A transmon quantum annealer: Decomposing many-body ising constraints into pair interactions*, 2016. DOI: 10.48550/ARXIV.1604.02359. [Online]. Available: https://arxiv.org/abs/1604.02359.

[102] P. K. Barkoutsos *et al.*, *Fermionic hamiltonians for quantum simulations: A general reduction scheme*, 2017. DOI: 10.48550/ARXIV.1706.03637. [Online]. Available: https://arxiv.org/abs/1706.03637.

[103] A. Teplukhin, B. K. Kendrick, and D. Babikov, "Calculation of molecular vibrational spectra on a quantum annealer," *Journal of Chemical Theory and Computation*, vol. 15, no. 8, pp. 4555–4563, Jul. 2019, ISSN: 1549-9626. DOI: 10.1021/acs.jctc.9b00402. [Online]. Available: http://dx.doi.org/10.1021/acs.jctc.9b00402.

[104] Y. Cao, R. Babbush, J. Biamonte, and S. Kais, "Hamiltonian gadgets with reduced resource requirements," *Physical Review A*, vol. 91, no. 1, Jan. 2015. DOI: 10.1103/physreva.91.012315. [Online]. Available: https://doi.org/10.1103%2Fphysreva.91.012315.

[105] Y. Cao and S. Kais, *Efficient optimization of perturbative gadgets*, Aug. 2017. DOI: 10.26421/qic17.9-10. [Online]. Available: https://doi.org/10.26421%2Fqic17.9-10.

[106] Y. Subaşı and C. Jarzynski, "Nonperturbative embedding for highly nonlocal hamiltonians," *Physical Review A*, vol. 94, no. 1, Jul. 2016. DOI: 10.1103/physreva.94.012342. [Online]. Available: https://doi.org/10.1103%2Fphysreva.94.012342.

[107] S. A. Ocko and B. Yoshida, "Nonperturbative gadget for topological quantum codes," *Physical Review Letters*, vol. 107, no. 25, Dec. 2011. DOI: 10.1103/physrevlett.107.250502. [Online]. Available: https://doi.org/10.1103%2Fphysrevlett.107.250502.

[108] R. Babbush, B. O'Gorman, and A. Aspuru-Guzik, "Resource efficient gadgets for compiling adiabatic quantum optimization problems," *Annalen der Physik*, vol. 525, no. 10-11, pp. 877–888, 2013.

[109] M. S. Anis *et al.*, *Qiskit: An open-source framework for quantum computing*, 2021. DOI: 10.5281/zenodo.2573505.

[110] J. Johansson, P. Nation, and F. Nori, "Qutip 2: A python framework for the dynamics of open quantum systems," *Computer Physics Communications*, vol. 184, no. 4, pp. 1234–1240, 2013, ISSN: 0010-4655. DOI: https://doi.org/10.1016/j.cpc.2012.11.019. [Online]. Available: https://www.sciencedirect.com/science/article/pii/S0010465512003955.

[111] Q. Sun *et al.*, "Pyscf: The python-based simulations of chemistry framework," *WIREs Computational Molecular Science*, vol. 8, no. 1, e1340, 2018. DOI: https://doi.org/10.1002/wcms.1340. eprint: https://wires.onlinelibrary.wiley.com/doi/pdf/10.1002/wcms.1340. [Online]. Available: https://wires.onlinelibrary.wiley.com/doi/abs/10.1002/wcms.1340.

[112] Y.-C. Yang, S. N. Coppersmith, and M. Friesen, "High-fidelity single-qubit gates in a strongly driven quantum-dot hybrid qubit with $1/f$ charge noise," *Physical Review A*, vol. 100, no. 2, Aug. 2019. DOI: 10.1103/physreva.100.022337. [Online]. Available: https://doi.org/10.1103%2Fphysreva.100.022337.

[113] J. L. Dodd, M. A. Nielsen, M. J. Bremner, and R. T. Thew, "Universal quantum computation and simulation using any entangling hamiltonian and local unitaries," *Physical Review A*, vol. 65, no. 4, Apr. 2002. DOI: 10.1103/physreva.65.040301. [Online]. Available: https://doi.org/10.1103%2Fphysreva.65.040301.

[114] S. Krinner *et al.*, *Realizing repeated quantum error correction in a distance-three surface code*, 2021. DOI: 10.48550/ARXIV.2112.03708. [Online]. Available: https://arxiv.org/abs/2112.03708.

[115] A. D. Córcoles *et al.*, "Demonstration of a quantum error detection code using a square lattice of four superconducting qubits," *Nature Communications*, vol. 6, no. 1, p. 6979, Apr. 2015, ISSN: 2041-1723. DOI: 10.1038/ncomms7979. [Online]. Available: https://doi.org/10.1038/ncomms7979.

[116] M. Urbanek, B. Nachman, V. R. Pascuzzi, A. He, C. W. Bauer, and W. A. de Jong, "Mitigating depolarizing noise on quantum computers with noise-estimation circuits," *Physical Review Letters*, vol. 127, no. 27, Dec. 2021. DOI: 10.1103/physrevlett.127.270502. [Online]. Available: https://doi.org/10.1103%2Fphysrevlett.127.270502.

[117] P. García-Molina, A. Martin, and M. Sanz, "Noise in digital and digital-analog quantum computation," *arXiv preprint arXiv:2107.12969*, 2021.

[118] C. Rigetti and M. Devoret, "Fully microwave-tunable universal gates in superconducting qubits with linear couplings and fixed transition frequencies," *Phys. Rev. B*, vol. 81, p. 134 507, 13 Apr. 2010. DOI: 10.1103/PhysRevB.81.134507. [Online]. Available: https://link.aps.org/doi/10.1103/PhysRevB.81.134507.

[119] O. G. Maupin, A. D. Baczewski, P. J. Love, and A. J. Landahl, "Variational quantum chemistry programs in JaqalPaq," en, *Entropy (Basel)*, vol. 23, no. 6, p. 657, May 2021.

[120] P. O'Malley *et al.*, "Scalable quantum simulation of molecular energies," *Physical Review X*, vol. 6, no. 3, Jul. 2016. DOI: 10.1103/physrevx.6.031007. [Online]. Available: https://doi.org/10.1103%2Fphysrevx.6.031007.

[121] S. Bravyi, J. M. Gambetta, A. Mezzacapo, and K. Temme, *Tapering off qubits to simulate fermionic hamiltonians*, 2017. DOI: 10.48550/ARXIV.1701.08213. [Online]. Available: https://arxiv.org/abs/1701.08213.

[122] J. A. Nelder and R. Mead, "A Simplex Method for Function Minimization," *The Computer Journal*, vol. 7, no. 4, pp. 308–313, Jan. 1965, ISSN: 0010-4620. DOI: 10.1093/comjnl/7.4.308. eprint: https://academic.oup.com/comjnl/article-pdf/7/4/308/1013182/7-4-308.pdf. [Online]. Available: https://doi.org/10.1093/comjnl/7.4.308.

[123] J. Romero, R. Babbush, J. R. McClean, C. Hempel, P. J. Love, and A. Aspuru-Guzik, "Strategies for quantum computing molecular energies using the unitary coupled cluster ansatz," *Quantum Science and Technology*, vol. 4, no. 1, p. 014 008, Oct. 2018. DOI: 10.1088/2058-9565/aad3e4. [Online]. Available: https://doi.org/10.1088/2058-9565/aad3e4.

[124] C. Cao *et al.*, *Towards a larger molecular simulation on the quantum computer: Up to 28 qubits systems accelerated by point group symmetry*, 2021. DOI: 10.48550/ARXIV.2109.02110. [Online]. Available: https://arxiv.org/abs/2109.02110.

[125] K. Setia, R. Chen, J. E. Rice, A. Mezzacapo, M. Pistoia, and J. D. Whitfield, "Reducing qubit requirements for quantum simulations using molecular point group symmetries," *Journal of Chemical Theory and Computation*, vol. 16, no. 10, pp. 6091–6097, Aug. 2020. DOI: 10.1021/acs.jctc.0c00113. [Online]. Available: https://doi.org/10.1021%2Facs.jctc.0c00113.

[126] M. Rossmannek, P. K. Barkoutsos, P. J. Ollitrault, and I. Tavernelli, "Quantum HF/DFT-embedding algorithms for electronic structure calculations: Scaling up to complex molecular systems," *The Journal of Chemical Physics*, vol. 154, no. 11, p. 114 105, Mar. 2021. DOI: 10.1063/5.0029536. [Online]. Available: https://doi.org/10.1063%2F5.0029536.

[127] N. C. Rubin, *A hybrid classical/quantum approach for large-scale studies of quantum systems with density matrix embedding theory*, 2016. DOI: 10.48550/ARXIV.1610.06910. [Online]. Available: https://arxiv.org/abs/1610.06910.

[128] F. Verstraete and J. I. Cirac, "Mapping local hamiltonians of fermions to local hamiltonians of spins," *Journal of Statistical Mechanics: Theory and Experiment*, vol. 2005, no. 09, P09012–P09012, Sep. 2005. DOI: 10.1088/1742-5468/2005/09/p09012. [Online]. Available: https://doi.org/10.1088%2F1742-5468%2F2005%2F09%2Fp09012.

[129] M. Steudtner and S. Wehner, "Fermion-to-qubit mappings with varying resource requirements for quantum simulation," *New Journal of Physics*, vol. 20, no. 6, p. 063 010, Jun. 2018. DOI: 10.1088/1367-2630/aac54f. [Online]. Available: https://doi.org/10.1088/1367-2630/aac54f.

[130] J. D. Whitfield, V. Havlíček, and M. Troyer, "Local spin operators for fermion simulations," *Physical Review A*, vol. 94, no. 3, Sep. 2016. DOI: 10.1103/physreva.94.030301. [Online]. Available: https://doi.org/10.1103%2Fphysreva.94.030301.

[131] Y.-A. Chen and Y. Xu, *Equivalence between fermion-to-qubit mappings in two spatial dimensions*, 2022. DOI: 10.48550/ARXIV.2201.05153. [Online]. Available: https://arxiv.org/abs/2201.05153.

[132] Z. Jiang, J. McClean, R. Babbush, and H. Neven, "Majorana loop stabilizer codes for error mitigation in fermionic quantum simulations," *Physical Review Applied*, vol. 12, no. 6, Dec. 2019. DOI: 10.1103/physrevapplied.12.064041. [Online]. Available: https://doi.org/10.1103%2Fphysrevapplied.12.064041.

[133] C. Derby, J. Klassen, J. Bausch, and T. Cubitt, "Compact fermion to qubit mappings," *Physical Review B*, vol. 104, no. 3, Jul. 2021. DOI: 10.1103/physrevb.104.035118. [Online]. Available: https://doi.org/10.1103%2Fphysrevb.104.035118.

[134] V. A. Rassolov and S. Garashchuk, "Computational complexity in quantum chemistry," *Chemical Physics Letters*, vol. 464, no. 4, pp. 262–264, 2008, ISSN: 0009-2614. DOI: https://doi.org/10.1016/j.cplett.2008.09.026. [Online]. Available: https://www.sciencedirect.com/science/article/pii/S0009261408012773.

[135] J. D. Whitfield, P. J. Love, and A. Aspuru-Guzik, "Computational complexity in electronic structure," *Phys. Chem. Chem. Phys.*, vol. 15, no. 2, pp. 397–411, 2013. DOI: 10.1039/c2cp42695a. [Online]. Available: https://doi.org/10.1039%2Fc2cp42695a.

[136] I. Kassal, S. P. Jordan, P. J. Love, M. Mohseni, and A. Aspuru-Guzik, "Polynomial-time quantum algorithm for the simulation of chemical dynamics," *Proceedings of the National Academy of Sciences*, vol. 105, no. 48, pp. 18 681–18 686, Dec. 2008. DOI: 10.1073/pnas.0808245105. [Online]. Available: https://doi.org/10.1073%2Fpnas.0808245105.

[137] J. D. Whitfield, M.-H. Yung, D. G. Tempel, S. Boixo, and A. Aspuru-Guzik, "Computational complexity of time-dependent density functional theory," *New Journal of Physics*, vol. 16, no. 8, p. 083 035, Aug. 2014. DOI: 10.1088/1367-2630/16/8/083035. [Online]. Available: https://doi.org/10.1088%2F1367-2630%2F16%2F8%2F083035.